104. Nicolson GL: Paracrine and autocrine growth mechanisms in tumor metastasis to specific sites with particular emphasis on brain and lung metastasis. *Cancer Metastasis Rev.* 12(3–4), 325–343 (1993).

105. Chinni SR, Sivalogan S, Dong Z *et al.*: CXCL12/CXCR4 signaling activates Akt-1 and MMP-9 expression in prostate cancer cells: the role of bone microenvironment-associated CXCL12. *Prostate* 66(1), 32–48 (2006).

106. Muller A, Homey B, Soto H *et al.*: Involvement of chemokine receptors in breast cancer metastasis. *Nature* 410(6824), 50–56 (2001).

▪ **Demonstrates that chemokine receptors including CXCR4 is involved in metastasis of breast cancer.**

107. Kim SY, Lee CH, Midura BV *et al.*: Inhibition of the CXCR4/CXCL12 chemokine pathway reduces the development of murine pulmonary metastases. *Clin. Exp. Metastasis* 25(3), 201–211 (2008).

108. Wong D, Korz W: Translating an antagonist of chemokine receptor CXCR4: from bench to bedside. *Clin. Cancer Res.* 14(24), 7975–7980 (2008).

109. Kajiyama H, Shibata K, Terauchi M, Ino K, Nawa A, Kikkawa F: Involvement of SDF-1α/CXCR4 axis in the enhanced peritoneal metastasis of epithelial ovarian carcinoma. *Int. J. Cancer* 122(1), 91–99 (2008).

110. Murakami T, Maki W, Cardones AR *et al.*: Expression of CXC chemokine receptor-4 enhances the pulmonary metastatic potential of murine B16 melanoma cells. *Cancer Res.* 62(24), 7328–7334 (2002).

111. Yoon Y, Liang Z, Zhang X *et al.*: CXC chemokine receptor-4 antagonist blocks both growth of primary tumor and metastasis of head and neck cancer in xenograft mouse models. *Cancer Res.* 67(15), 7518–7524 (2007).

112. Sun YX, Schneider A, Jung Y *et al.*: Skeletal localization and neutralization of the SDF-1(CXCL12)/CXCR4 axis blocks prostate cancer metastasis and growth in osseous sites *in vivo*. *J. Bone Miner. Res.* 20(2), 318–329 (2005).

113. Smith MC, Luker KE, Garbow JR *et al.*: CXCR4 regulates growth of both primary and metastatic breast cancer. *Cancer Res.* 64(23), 8604–8612 (2004).

114. Iwasaki Y, Akari H, Murakami T *et al.*: Efficient inhibition of SDF-1α-mediated chemotaxis and HIV-1 infection by novel CXCR4 antagonists. *Cancer Sci.* 100(4), 778–781 (2009).

115. Zhou Y, Larsen PH, Hao C, Yong VW: CXCR4 is a major chemokine receptor on glioma cells and mediates their survival. *J. Biol. Chem.* 277(51), 49481–49487 (2002).

116. Rubin JB, Kung AL, Klein RS *et al.*: A small-molecule antagonist of CXCR4 inhibits intracranial growth of primary brain tumors. *Proc. Natl Acad. Sci. USA* 100(23), 13513–13518 (2003).

117. Tamamura H, Fujii N: The therapeutic potential of CXCR4 antagonists in the treatment of HIV infection, cancer metastasis and rheumatoid arthritis. *Expert Opin. Ther. Targets* 9(6), 1267–1282 (2005).

118. Xiao Q, Ye S, Oberhollenzer F *et al.*: SDF1 gene variation is associated with circulating SDF1α level and endothelial progenitor cell number: the Bruneck Study. *PLoS ONE* 3(12), e4061 (2008).

119. Cashen A, Lopez S, Gao F *et al.*: A Phase II study of plerixafor (AMD3100) plus G-CSF for autologous hematopoietic progenitor cell mobilization in patients with Hodgkin lymphoma. *Biol. Blood Marrow Transplant.* 14(11), 1253–1261 (2008).

▪ **Shows a successful result from the Phase II study of hematopoietic progenitor cell mobilization by AMD3100.**

120. Nakata H, Steinberg SM, Koh Y *et al.*: Potent synergistic anti-human immunodeficiency virus (HIV) effects using combinations of the CCR5 inhibitor aplaviroc with other anti-HIV drugs. *Antimicrob. Agents Chemother.* 52(6), 2111–2119 (2008).

121. Reeves JD, Gallo SA, Ahmad N *et al.*: Sensitivity of HIV-1 to entry inhibitors correlates with envelope/coreceptor affinity, receptor density, and fusion kinetics. *Proc. Natl Acad. Sci. USA* 99(25), 16249–16254 (2002).

122. Reeves JD, Miamidian JL, Biscone MJ *et al.*: Impact of mutations in the coreceptor binding site on human immunodeficiency virus type 1 fusion, infection, and entry inhibitor sensitivity. *J. Virol.* 78(10), 5476–5485 (2004).

123. Nagasawa T, Hirota S, Tachibana K *et al.*: Defects of B-cell lymphopoiesis and bone-marrow myelopoiesis in mice lacking the CXC chemokine PBSF/SDF-1. *Nature* 382(6592), 635–638 (1996).

124. Tachibana K, Hirota S, Iizasa H *et al.*: The chemokine receptor CXCR4 is essential for vascularization of the gastrointestinal tract. *Nature* 393(6685), 591–594 (1998).

125. Zou YR, Kottmann AH, Kuroda M, Taniuchi I, Littman DR: Function of the chemokine receptor CXCR4 in haematopoiesis and in cerebellar development. *Nature* 393(6685), 595–599 (1998).

Website

201. UNAIDS www.unaids.org/en/HIV_data/

Remodeling of Dynamic Structures of HIV-1 Envelope Proteins Leads to Synthetic Antigen Molecules Inducing Neutralizing Antibodies

Toru Nakahara,[†] Wataru Nomura,*[,†] Kenji Ohba,[‡] Aki Ohya,[†] Tomohiro Tanaka,[†] Chie Hashimoto,[†] Tetsuo Narumi,[†] Tsutomu Murakami,[‡] Naoki Yamamoto,[‡] and Hirokazu Tamamura*[,†]

Department of Medicinal Chemistry, Institute of Biomaterials and Bioengineering, Tokyo Medical and Dental University, 2-3-10 Kandasurugadai, Chiyoda-ku, Tokyo 101-0062, Japan, and AIDS Research Center, National Institute of Infectious Diseases, 1-23-1 Toyama, Shinjuku-ku, Tokyo 162-8640, Japan. Received November 16, 2009; Revised Manuscript Received February 28, 2010

A synthetic antigen targeting membrane-fusion mechanism of HIV-1 has a newly designed template with C3-symmetric linkers mimicking N36 trimeric form. The antiserum produced by immunization of the N36 trimeric form antigen showed structural preference in binding to N36 trimer and stronger inhibitory activity against HIV-1 infection than the N36 monomer. Our results suggest an effective strategy of HIV vaccine design based on a relationship to the native structure of proteins involved in HIV fusion mechanisms.

INTRODUCTION

Antibody-based therapy is one of the promising treatments for AIDS. In recent years, AIDS antibodies have been produced by immunization (*1*) and by de novo engineering of monoclonal antibodies (mAb) with molecular evolution tactics such as phage display (*2*). Despite enormous efforts, however, only a limited number of highly and broadly HIV-neutralizing human mAbs have been isolated and characterized. These antibodies include gp41 Abs, 2F5 (*3*−*6*) and 4E10 (*5*−*7*), and gp120 Abs, 2G12 (*8*) and b12 (*9*). gp41 is a transmembrane envelope glycoprotein, which is divided into an endodomain and an ectodomain by the transmembrane region; the latter contains a hydrophobic amino-terminal fusion peptide, followed by amino-terminal and carboxy-terminal leucine/isoleucine heptad repeat domains with helical structures (HR1 and HR2, respectively). In the membrane fusion process of HIV-1, these subunits form a "pre-bundle" complex. The HR1 and HR2 regions are termed the N-terminal helix (N36) and C-terminal helix (C34), respectively. These helices form a six-helical bundle consisting of a central parallel trimeric coiled-coil of N36 surrounded by C34 in an antiparallel hairpin fashion. In design of immunogens that elicit broadly neutralizing antibodies, a useful strategy is to produce molecules that mimic the natural trimer on the virion surface. Previous studies show that these molecules could be proteins expressed as a recombinant form or on the surface of particles such as pseudovirions or proteoliposomes (*10*−*12*). The X-ray crystallographic study of gp41 shows that the distances between any two residues at the N-terminus of N-region are almost equal at approximately 10 Å (Figure 1A). A chemically synthetic template could be useful in connection with the design of a peptidomimetic corresponding to the native structure of gp41. To date, several gp41 mimetics have been synthesized as inhibitors or antigens and subjected to inhibition or neutralization assays (*13*−*16*). However, the templates for assembly of these helical peptides contain branched peptide linkers, which are not exactly equivalent in length (*14*). The N-terminal peptides constrained by another threefold linker showed high affinity for C-terminal peptides, although its biological advantages have not been determined (*15*). The mimicry can be estimated using the broadly neutralizing mAbs; suitable mimetics will bind neutralizing mAbs efficiently, but they will bind non-neutralizing mAbs poorly. In the present study, we designed and synthesized a novel three-helical bundle mimetic, which corresponds to the trimeric form of N36. We investigated whether mice immunized with the equivalent trimeric form of N36 mimetic can produce antibodies with stronger binding affinity for N36 trimer than for N36 monomer. This approach demonstrates the possibility of producing structure-specific antibodies by immunization of synthetic antigens corresponding to the natural form of viral proteins.

* To whom correspondence should be addressed. E-mail: nomura.mr@tmd.ac.jp; tamamura.mr@tmd.ac.jp. phone: +81-3-5280-8036, fax: +81-3-5280-8039.

[†] Tokyo Medical and Dental University.

[‡] National Institute of Infectious Diseases.

EXPERIMENTAL PROCEDURES

Conjugation of N36REGC and the Template to Produce triN36e. Compound **6** (100 μg, 0.174 μmol) and N36REGC (3.4 mg, 0.574 μmol) were dissolved in a mixture of 300 μL of 200 mM acetate buffer (pH 5.2) and 300 μL of TFE under a nitrogen atmosphere, then TCEP·HCl was added. The reaction was stirred for 72 h at room temperature and monitored by HPLC. The ligation product (triN36e) was separated as an HPLC peak and was characterized by ESI-TOF-MS, *m/z* calcd for $C_{690}H_{1160}N_{226}O_{201}S_3$ 15933.1, found 15933.8. The purification was performed by reverse phase HPLC (YMC-Pack ODS-A column, 10 × 250 mm). Elution was carried out with a 40−50% linear gradient of acetonitrile (0.1% TFA) over 50 min. Purified triN36e, obtained in 16% yield, was identified by ESI-TOF-MS. The detailed synthesis of peptides is described in the Supporting Information (SI).

CD Spectra. CD measurements were performed with a J-720 circular dichroism spectrolarimeter equipped with a thermoregulator (JASCO). The wavelength dependence of molar ellipticity [θ] was monitored at 25 °C from 190 to 250 nm. Peptides were dissolved in 20 mM acetate buffer (pH 4.0) containing 40% MeOH (*23, 24*). The experimental helicity was calculated as reported previously (*17*−*19*).

Immunization and Sample Collection. Six-week-old male BALB/c mice were purchased from Sankyo Laboratory Service Corp. (Tokyo, Japan) and maintained under specific pathogen-free conditions in an animal facility. The experimental protocol was approved by the ethical review committee of Tokyo Medical and Dental University. Freund incomplete adjuvant and PBS

10.1021/bc900502z
Published on Web 04/01/2010

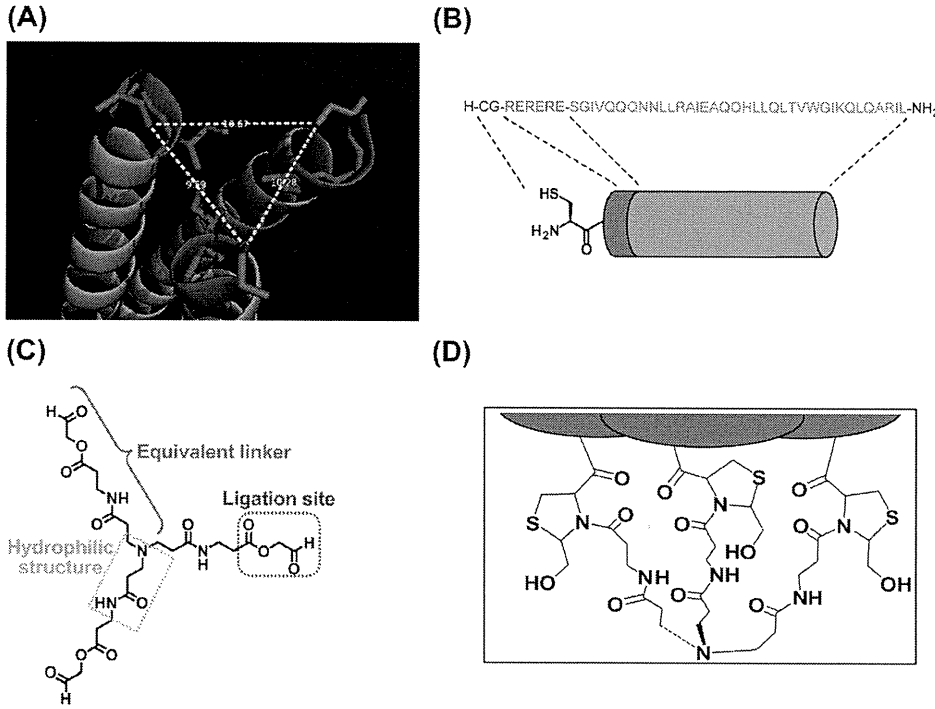

Figure 1. (A) Distances between hydrogen atoms for hydroxyl groups in N-terminal serine residues of N36 helices in trimeric form. The distances were evaluated by PyMOL (*21*). (B) Cartoon presentation of each N36 derived peptide, N36REGC. (C) Design of a C3-symmetric template. The amino acid residues are described in single letters. (D) Conjugated structure of trimeric N36 after thiazolidine ligation.

were purchased from Wako Pure Chemical Industries (Osaka, Japan). DMSO (endotoxin free) was purchased from Sigma-Aldrich (St. Louis, MO).

All mice were bled one week before immunization. One hundred micrograms of antigen was dissolved in 1 μL of DMSO. The solution was mixed with 50 μL of PBS and 50 μL of Freund incomplete adjuvant. The mixture was injected subcutaneously under anesthesia on days 0, 14, 28, 42, and 58. Mice were bled on days 21, 35, 49, and 65. Serum was separated by centrifugation (15 000 rpm) at 4 °C for 15 min and inactivated at 56 °C for 30 min. Sera were stored at −80 °C before use.

Serum Titer ELISA. Tween-20 (polyoxyethylene (20) sorbitan monolaurate) and hydrogen peroxide (30%) were purchased from Wako. ABTS (2,2-azino-bis(3-ethylbenzothiazoline-6-sulfonic acid) diammonium salt) was purchased from Sigma-Aldrich. Antimouse IgG (H+L)(goat)-HRP was purchased from EMD Chemicals (San Diego, CA). Ninty-six-well microplates were coated with 25 μL of a synthetic peptide at 10 μg/mL in PBS at 4 °C for overnight. The coated plates were washed 10 times with deionized water and blocked with 150 μL of blocking buffer (0.02% PBST, PBS with 0.02% Tween 20, containing 5% skim milk) at 37 °C for 1 h. The plates were washed with deionized water 10 times. Mice sera were diluted in 0.02% PBST with 1% skim milk, and 50 μL of 2-fold serial dilutions of sera from 1/200 to 1/102400 were added to the wells and allowed to incubate at 37 °C for 2 h. The plates were washed 10 times with deionized water. Twenty-five microliters of HRP-conjugated antimouse IgG, diluted 1:2000 in 0.02% PBST, was added to each well. After 45 min incubation, the plates were washed 10 times and 25 μL of HRP substrate, prepared by dissolving 10 mg ABTS to 200 μLof HRP staining buffer—a mixture of 0.5 M citrate buffer (pH 4.0, 1 mL), H_2O_2 (3 μL), and H_2O (8.8 mL)—was added. After 30 min incubation, the reaction was stopped by addition of 25 μL/well 0.5 M H_2SO_4, and optical densities were measured at 405 nm.

Virus Preparation. The pNL4-3 construct (8 μg) was transfected into 293T cells by Lipofectamine LTX (Invitrogen, Carlsbad, CA) followed by changing medium at 12 h after transfection. At 48 h after changing medium, the supernatant was collected, passed through a 0.45 μm filter, and stored at −80 °C as HIV-1_{NL4-3} strain before use. For titration, MT-4 cells were infected with serially 3-fold diluted virus from 1/10 to 1/196830, and cultured for 7 days. HIV-1 p24 levels in supernatants were measured, and then the titer of virus solution was calculated.

Anti-HIV Assay. Virus was prepared as described above except that the transfection of pNL4-3 was performed by the calcium phosphate method. Anti-HIV-1 activity was determined on the basis of protection against HIV-1-induced cytopathogenicity in MT-4 cells. Various concentrations of AZT, N36RE, and triN36e (The starting concentrations are 100, 10, and 1 μM, respectively) were added to HIV-1-infected MT-4 cells (MOI = 0.01) by 2-fold serial dilution and placed in wells of a flat-bottomed microtiter plate (2.0×10^4 cells/well). After 5 days' incubation at 37 °C in a CO_2 incubator, the number of viable cells was determined using the 3-(4,5-dimethylthiazol-2-yl)-2,5-diphenyltetrazolium bromide (MTT) method (EC_{50}). Cytotoxicity of compounds was determined on the basis of viability of mock-infected cells using the MTT method (CC_{50}). Each experiment was performed three times independently.

Neutralizing Assay. MT4-cells (1×10^5 cells/100 μL) were incubated in 100 μL medium containing 10 μL sera from immunized or preimmunized mice for 1 h at 37 °C, then pretreated MT-4 cells were infected with HIV-1_{NL4-3} (MOI = 0.05). At 3 days after infection, cells were collected by centrifuge at 4000 rpm for 10 min at 4 °C. After discarding supernatant, pellets were lysed with 30 μL of lysis buffer (50 mM Tris·HCl (pH 7.5), 150 mM NaCl, 1% NP-40), then 30 μL of 2 × SDS buffer (125 mM Tris·HCl (pH 6.8), 4% SDS, 20% glycerol, 10% 2-ME, 0.004% BPB) were added and boiled for 10 min. The samples (5 μL) were subjected to SDS-page to perform Western blotting. The HIV-1 gag p24 was detected by using Western lightning ECL kit (PerkinElmer, MA) according to manufacturer's instruction after treatment of HIV-1 p24

Scheme 1. Synthesis of the Equivalently Branched Template 6

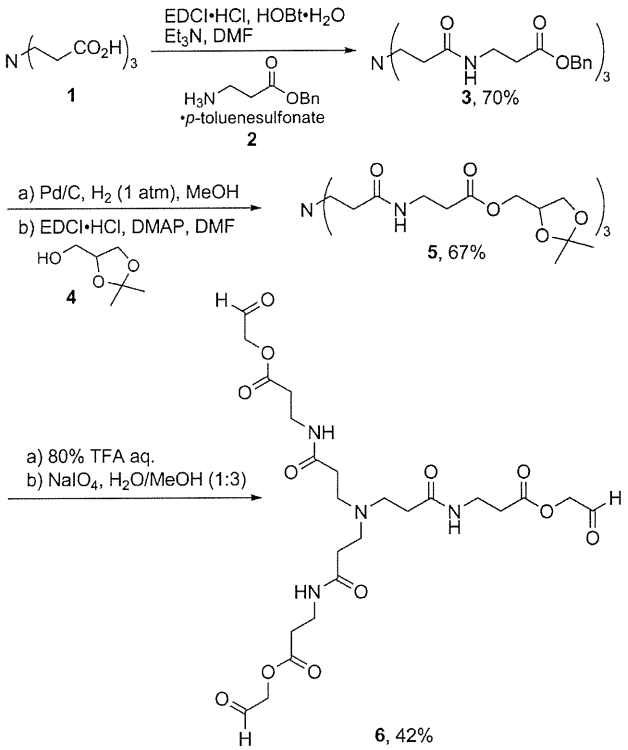

antibody (2C2; 1:2000 dilution) (*20*) and anti- mouse IgG (H+L)-HRP (Millipore, MA). The band intensity of p24 was calculated with post/pre-immunized samples by using *ImageJ* image analyzing software.

RESULTS AND DISCUSSION

The N-region of gp41 is known to be an aggregation site involving a trimeric coiled-coil conformation. In design of an N36-derived peptide (N36RE), the triplet repeat of arginine and glutamic acid was fused to the N-terminus to increase the solubility in buffer solution (Figure 1B). In order to form a triple helix corresponding precisely to the gp41 prefusion form, we designed the novel C3-symmetric template depicted in Figure 1C. This designed template linker has three branches of equal length and possesses the hydrophilic structure and ligation site for coupling with N36RE. The template was synthesized from the commercially available 3-[bis(2-carboxyethyl)amino]propanoic acid **1** as shown in Scheme 1. Coupling of **1** with β-alanine benzyl ester **2** gave the corresponding triamide **3** in 77% yield. Cleavage of three benzyl esters by hydrogenation and coupling with solketal **4** produced the corresponding triester **5**. Deprotection of the acetonides with aqueous 80% TFA followed by oxidative cleavage of diol group led to the desired template **6**. This approach uses thiazolidine ligation for chemoselective coupling of Cys-containing unprotected N36RE (N36REGC) with a three-armed aldehyde scaffold producing triN36e (Figure 1D). Thiazolidine ligation is a peptide segment coupling strategy which does not require side chain protecting groups (*22*−*26*). The reaction consists of three steps: (i) aldehyde introduction, in which a masked glycolaldehyde ester is linked to the carboxyl terminus of an unprotected peptide by reverse proteolysis; (ii) ring formation, in which the unmasked aldehyde reacts at acidic pH with the α-amino group of an N-terminal cysteine residue of the second unprotected peptide forming a thiazolidine ring; and (iii) rearrangement at higher pH in which O-acyl ester linkage is converted to an N-acyl amide linkage forming a peptide bond with a pseudoproline structure (Figure 2).

Circular dichroism (CD) spectra of triN36e and N36RE, which is a monomer form without N-terminal Cys-Gly residues, are shown in Figure 3A. The peptides were dissolved in 20 mM acetate buffer with 40% MeOH, pH4.0, suitable for measurement of CD spectra of membrane proteins (*27, 28*). Both spectra display double minima at 208 and 222 nm and showed high molar ellipticity as absolute values (Table 1). The results indicate that these peptides form a highly structured α-helix and that the helical content of the trimer triN36e is higher than that of the monomer N36RE. Furthermore, to assess the interaction of triN36e with C34, CD spectra of the peptide mixture with C34-derived peptide, C34RE, were measured (Figure 3B,C). The spectrum of triN36e and C34RE mixture showed high molecular ellipticity as an absolute value comparable with that of triN36e alone. This supports the conclusion that C34RE interacts with tri36e and thereby induces a higher helical form as shown previously (*29*).

Mice were immunized with these synthetic gp41 mimetics and antibody production was successfully induced (the detailed titer increase in 5 weeks' immunization is given in the Supporting Information). Two out of three mice showed induction of antibodies against either antigen (N36RE or triN36e). Antibody titers and selectivity of antisera isolated from mice immunized with N36RE or triN36e were evaluated by serum titer ELISA against coated synthetic antigens. The most active antiserum for each antigen was utilized for the evaluation of binding activity by ELISA (Figure 4). The N36RE-induced antibody showed approximately 5 times higher affinity for N36RE than for triN36e, as 50% bound serum dilutions are 3.88×10^{-4} and 2.14×10^{-3} to N36RE and triN36e, respectively. It is noteworthy that the triN36e-induced antibody showed approximately 30 times higher preference in binding affinity for triN36e antigen than for N36RE (serum dilutions at 50% bound are 3.83×10^{-3} to N36RE and 1.33×10^{-4} to triN36e). Although this evaluation was not determined with purified mAbs, it is clear that the antibodies produced exploit a structural preference for antigens. The mechanism of induction

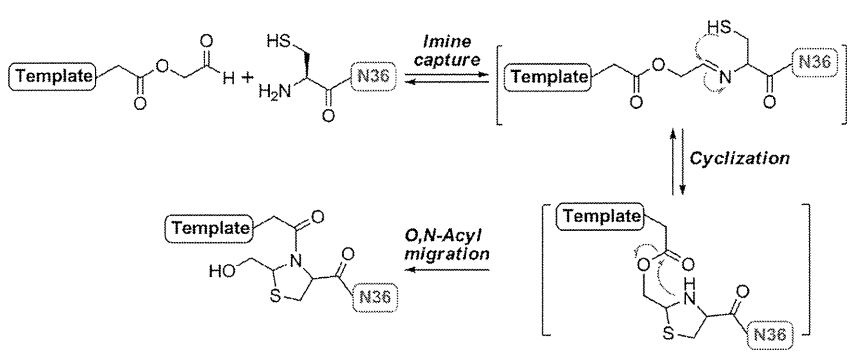

Figure 2. Reaction mechanisms of thiazolidine ligation utilized for assembly of N36RE helices on the template.

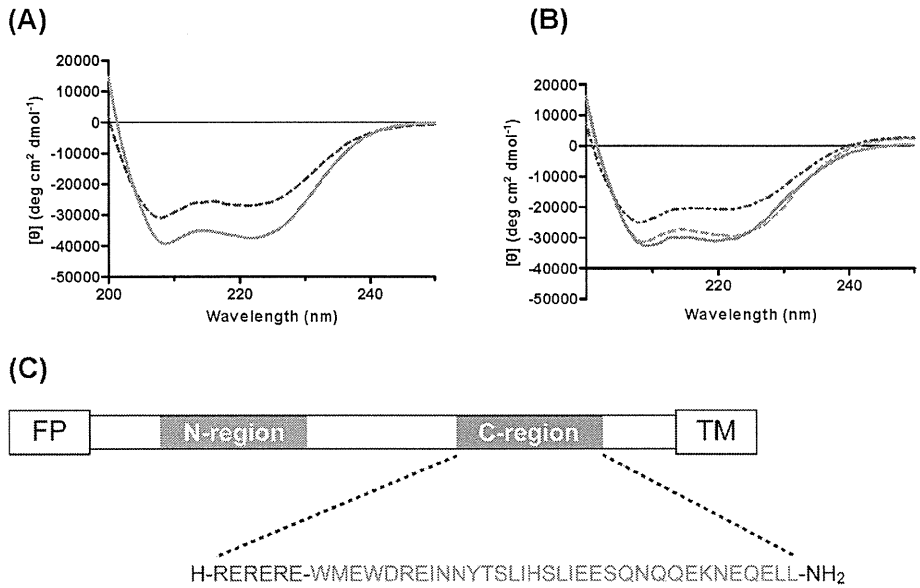

Figure 3. (A) Circular dichroism (CD) spectra of N36RE and triN36e. In the spectra, a blue dashed line and a green line show N36RE (monomer) and triN36e (trimer), respectively. Concentrations of the peptides are 10 and 3.3 μM for N36RE and triN36e, respectively. (B) CD spectra in the presence or absence of C34RE peptide. The spectra show the following: a dashed green line, triN36e; a dashed blue line, C34RE; a red line, triN36e+C34RE, respectively. The concentrations of peptides were as follows: triN36e (2.3 μM), C34-derived peptide C34RE (7 μM), and mixture of both peptides (3.5 μM each). (C) The amino acid sequence of C34RE described in single letters. FP and TM represent hydrophobic fusion peptide and transmembrane domain, respectively.

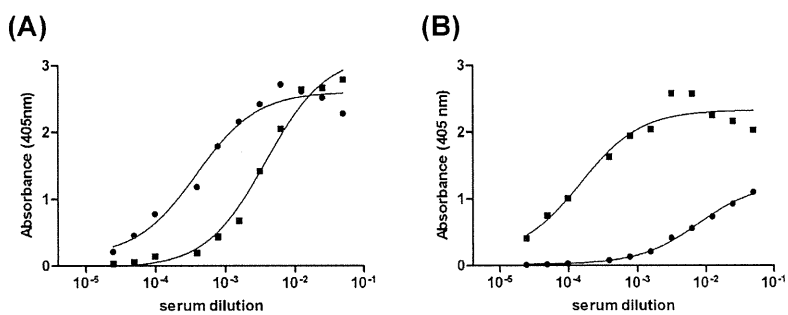

Figure 4. Serum titers of antibodies produced by N36 monomer and conformationally constrained N36 trimeric antigen. The titers were evaluated against N36RE (monomer) (A) and triN36e (trimer) (B). The plots indicate the results of sera obtained from N36RE-immunized mouse (•) and triN36e-immunized mouse (■).

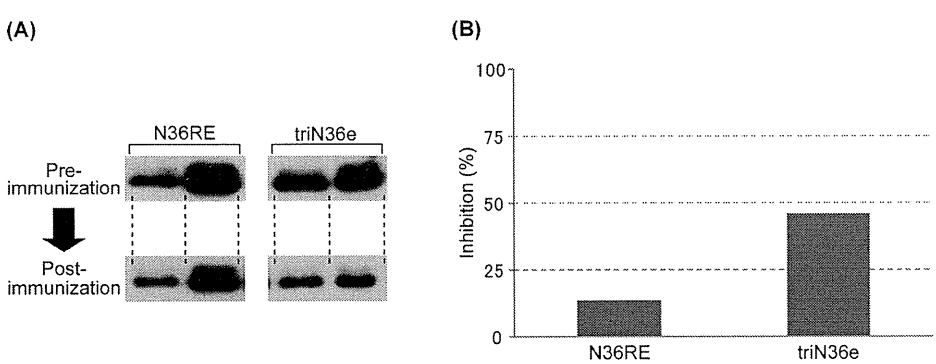

Figure 5. Determination of neutralization activity of the antibodies produced by immunization of peptidomimetic antigens. (A) Results of p24 assay to evaluate inhibition for HIV-1 infection by produced antibodies. Preimmunization sera were used as control. Experiments were duplicated. (B) Average % inhibition of p24 production calculated from the band intensities in panel (A).

of structure-specific antibody is still not clear, but the results could suggest the efficacy of producing antibodies with structural specificity and that the synthesis of structure-involving antigens is an effective strategy when higher specificity is required.

Neutralizing activity of sera against HIV-1 infection was assessed by p24 assays utilizing antisera from two mice that showed antibody production for each antigen (Figure 5). Sera

Table 1. Differences of α-Helicities between N36RE and triN36e Calculated from CD Spectra in Figure [3]

	$[\theta]_{222}$	$[\theta]_{222}/[\theta]_{208}$	α-helicity
N36RE	−30 957	0.87	73%
triN36e	−38 998	0.96	95%

Table 2. EC_{50} and CC_{50} Values Calculated from Inhibition Assays of Peptidomimetics

	AZT	triN36e	N36RE
EC_{50} (μM)[a]	0.047	0.49	1.4
CC_{50} (μM)[b]	>50	>1	>10

[a] EC_{50} values are based on the inhibition of HIV-induced cytopathogenicity in MT-4 cells. [b] CC_{50} values are based on the reduction of the viability of MT-4 cells. All data are the mean values for at least three experiments.

from mice immunized with the same antigen showed similar inhibitory activity against viral infection (12.5% and 14.8% for N36RE, 40.3% and 52.1% for triN36e). A trend was observed that the sera from triN36e immunization shows higher inhibition than those from N36RE immunization. This suggests that the synthetic antigen corresponding to the N36 trimeric form induces antibody with neutralization activity superior to that of the monomer peptide antigen and implies a restricted response of B-cells upon immunization to the trimeric form of N36RE. In order to assess the compatibility of induced antibodies in HIV-1 entry inhibition, the HIV-1 inhibitory activities of peptidomimetics (N36RE and triN36e) have been evaluated by viral infection and cytotoxicity assays. A C-terminal region peptide known as Enfuvirtide (T20, Roche/Trimeris) has been used clinically as a fusion inhibitor, and its success indicates that gp41-derived peptides might be potent inhibitors, useful against HIV-1 infection (*30*). In the development of anti-HIV peptides, several mimetics such as Enfuvirtide, CD4 binding site of gp120 (*31*), and protein-nucleic acid interactions (*32*), which disrupt protein−protein interactions, have been produced. As indicated in Table 2, N36 and triN36e showed modest inhibitory activity as reported in previous studies (*33*−*35*). The potency of triN36e was three times higher than that of N36RE indicating that the active structure of monomer N36RE is a trimeric form. Cytotoxicity of the antigens was not observed at concentrations of 1 μM of triN36e and 10 μM of N36RE.

CONCLUSIONS

In summary, a mimic of HIV-1 gp41-N36 designed as a new vaccine has been synthesized utilizing a novel template with three branched linkers of equal lengths. Thiazolidine-forming ligation attached the esteraldehyde of three-branched template with N-terminal cysteine of peptides in an aqueous medium. The resulting peptide antigen successfully induces antibodies with neutralization activity against HIV-1 infection. It is of special interest that the antibody produced acquires structural preference to antigen, which showed 30 times higher binding affinity for trimer than for monomer. This indicates the effectiveness of the design based on the structural dynamics of HIV-1 fusion mechanism of an antigen which could elicit neutralizing antibodies. In a design based on the N36 region of gp41, the exposed timing of epitopes is limited during HIV-1 entry (*36*), and carbohydrates, which could make accession of antibodies to epitopes difficult, are not associated with the amino acid residues of the native protein. These two advantages could further enhance the potential of a vaccine design based on the N36 region. During preparation of the manuscript, a new HIV vaccine strategy was reported by Burton's group (*37*). The report describes the importance of antibody recognition for the trimer form of surface protein. The trimer-specific antibodies indicate broad and potent neutralization. The gp41 trimer-form specific antibody produced in this study could also obtain the corresponding properties. The elucidation of antibody-producing mechanisms and epitope recognition mode of antibodies in antiserum during HIV-1 entry will be addressed in future studies.

ACKNOWLEDGMENT

The authors deeply thank Prof. K. Akiyoshi (Tokyo Medical and Dental Univ.) for allowing access to CD spectroporalimeter.

Supporting Information Available: HPLC chromatograms and NMR charts of compounds **3**, **5**, and **6**. Results of ESI-TOF-MS, and HPLC chromatograms of peptides N36RE, N36REGC, and triN36e. Results of serum titer ELISA of antisera collected during immunization. This material is available free of charge via the Internet at http://pubs.acs.org.

LITERATURE CITED

(1) Cabezas, E., Wang, M., Parren, P. W. H. I., Stanfield, R. L., and Satterthwait, A. C. (2000) A structure-based approach to a synthetic vaccine for HIV-1. *Biochemistry 39*, 14377–14391.

(2) Burton, D. R., Barbas, C. F., III, Persson, M. A. A., Koenig, S., Chanock, R. M., and Lerner, R. A. (1991) A large array of human monoclonal antibodies to type 1 human immunodeficiency virus from combinatorial libraries of asymptomatic seropositive individuals. *Proc. Natl. Acad. Sci. U.S.A. 88*, 10134–10137.

(3) Conley, A. J., Kessler, J. A. II, Boots, L. J., Tung, J. S., Arnold, B. A., Keller, P. M., Shaw, A. R., and Emini, R. A. (1994) Neutralization of divergent human immunodeficiency virus type 1 variants and primary isolates by IAM-41−2F5, an anti-gp41 human monoclonal antibody. *Proc. Natl. Acad. Sci. U.S.A. 91*, 3348–3352.

(4) Ofek, G., Tang, M., Sambor, A., Katinger, H., Mascola, J. R., Wyatt, R., and Kwong, P. D. (2004) Structure and mechanistic analysis of the anti-human immunodeficiency virus type 1 antibody 2F5 in complex with its gp41 epitope. *J. Virol. 78*, 10724–10737.

(5) Alam, S. M., McAdams, M., Boren, D., Rak, M., Scearce, R. M., Gao, F., Camacho, Z. T., Gewirth, D., Kelsoe, G., Chen, P., and Haynes, B. F. (2007) The role of antibody polyspecificity and lipid reactivity in binding of broadly neutralizing anti-HIV-1 envelope human monoclonal antibodies 2F5 and 4E10 to glycoprotein 41 membrane proximal envelope epitopes. *J. Immunol. 178*, 4424–4435.

(6) Nelson, J. D., Brunel, F. M., Jensen, R., Crooks, E. T., Cardoso, R. M. F., Wang, M., Hessell, A., Wilson, I. A., Binley, J. M., Dawson, P. E., Burton, D. R., and Zwick, M. B. (2007) An affinity-enhanced neutralizing antibody against the membrane-proximal external region of human immunodeficiency virus type 1 gp41 recognizes an epitope between those of 2F5 and 4E10. *J. Virol. 81*, 4033–4043.

(7) Cardoso, R. M. F., Zwick, M. B., Stanfield, R. L., Kunert, R., Binley, J. M., Katinger, H., Burton, D. R., and Wilson, I. A. (2005) Broadly neutralizing anti-HIV antibody 4E10 recognizes a helical conformation of a highly conserved fusion-associated motif in gp41. *Immunity 22*, 163–173.

(8) Trkola, A., Purtscher, M., Muster, T., Ballaun, C., Buchacher, A., Sullivan, N., Srinivasan, K., Sodroski, J., Moore, J. P., and Katinger, H. (1996) Human monoclonal antibody 2G12 defines a distinctive neutralization epitope on the gp120 glycoprotein of human immunodeficiency virus type 1. *J. Virol. 70*, 1100–1108.

(9) Pantophlet, R., Saphire, E. O., Poignard, P., Parren, P. W. H. I., Wilson, I. A., and Burton, D. R. (2003) Fine mapping of the interaction of neutralizing and nonneutralizing monoclonal antibodies with the CD4 binding site of human immunodeficiency virus type 1 gp120. *J. Virol. 77*, 642–658.

(10) Sanders, R. W., Vesanen, M., Schuelke, N., Master, A., Schiffner, L., Kalyanaraman, R., Paluch, M., Berkhout, B., Maddon, P. J., Olson, W. C., Lu, M., and Moore, J. P. (2002) Stabilization of the soluble, cleaved, trimeric form of the envelope glycoprotein complex of human immunodeficiency virus type 1. *J. Virol. 76*, 8875–8889.

(11) Yang, X., Wyatt, R., and Sodroski, J. (2001) Improved elicitation of neutralizing antibodies against primary human immunodeficiency viruses by soluble stabilized envelope glycoprotein trimers. *J. Virol. 75*, 1165–1171.
(12) Grundner, C., Mirzabekov, T., Sodroski, J., and Wyatt, R. (2002) Solid-phase proteoliposomes containing human immunodeficiency virus envelope glycoproteins. *J. Virol. 76*, 3511–3521.
(13) De Rosny, E., Vassell, R., Wingfield, R. T., Wild, C. T., and Weiss, C. D. (2001) Peptides corresponding to the heptad repeat motifs in the transmembrane protein (gp41) of human immunodeficiency virus type 1 elicit antibodies to receptor-activated conformations of the envelope glycoprotein. *J. Virol. 75*, 8859–8863.
(14) Tam, J. P., and Yu, Q. (2002) A facile ligation approach to prepare three-helix bundles of HIV fusion-state protein mimetics. *Org. Lett. 4*, 4167–4170.
(15) Xu, W., and Taylor, J. W. (2007) A template-assembled model of the N-peptide helix bundle from HIV-1 gp-41 with high affinity for C-peptide. *Chem. Biol. Drug Des. 70*, 319–328.
(16) Louis, J. M., Nesheiwat, I., Chang, L., Clore, G. M., and Bewlet, C. A. (2003) Covalent trimers of the internal N-terminal trimeric coiled-coil of gp41 and antibodies directed against them are potent inhibitors of HIV envelope-mediated cell fusion. *J. Biol. Chem. 278*, 20278–20285.
(17) Chen, Y.-H., Yang, J. T., and Chau, K. H. (1974) Determination of the helix and β form of proteins in aqueous solution by circular dichroism. *Biochemistry 13*, 3350–3359.
(18) Gans, P. J., Lyu, P. C., Manning, M. C., Woody, R. W., and Kallenbach, N. R. (1991) The helix-coil transition in heterogeneous peptides with specific side-chain interactions: theory and comparison with CD spectral data. *Biopolymers 13*, 1605–1614.
(19) Jackson, D. Y., King, D. S., Chmielewski, J., Singh, S., and Schultz, P. G. (1991) A general approach to the synthesis of short alpha-helical peptides. *J. Am. Chem. Soc. 113*, 9391–9392.
(20) Ohba, K., Ryo, A., Dewan, M. Z., Nishi, M., Naito, T., Qi, X., Inagaki, Y., Nagashima, Y., Tanaka, Y., Okamoto, T., Terashima, K., and Yamamoto, N. (2009) Follicular dendritic cells activate HIV-1 replication in monocytes/macrophages through a juxtacrine mechanism mediated by P-selectin glycoprotein ligand 1. *J. Immunol. 183*, 524–532.
(21) Liu, J., Shu, W., Fagan, M. B., Nunberg, J. H., and Lu, H. (2001) Structural and functional analysis of the HIV gp41 core containing an Ile573 to Thr substitution: implications for membrane fusion. *Biochemistry 40*, 2797–2807.
(22) Liu, C. F., and Tam, J. P. (1994) Peptide segment ligation strategy without use of protecting groups. *Proc. Natl. Acad. Sci. U.S.A. 91*, 6584–6588.
(23) Tam, J. P., and Miao, Z. (1999) Stereospecific pseudoproline ligation of N-terminal serine, threonine, or cysteine-containing unprotected peptides. *J. Am. Chem. Soc. 121*, 9013–9022.
(24) Tam, J. P., Yu, Q., and Yang, J.-L. (2001) Tandem ligation of unprotected peptides through thiaprolyl and cysteinyl bonds in water. *J. Am. Chem. Soc. 123*, 2487–94.
(25) Eom, K. D., Miao, Z., Yang, J.-L., and Tam, J. P. (2003) Tandem ligation of multipartite peptides with cell-permeable activity. *J. Am. Chem. Soc. 125*, 73–82.
(26) Sadler, K., Zhang, Y., Xu, J., Yu, Q., and Tam, J. P. (2008) Quaternary protein mimetics of gp41 elicit neutralizing antibodies against HIV fusion-active intermediate state. *Biopolym. (Pept. Sci.) 90*, 320–329.
(27) Bychkova, V. E., Dujsekina, A. E., Klenin, S. I., Tiktopulo, E. I., Uversky, V. N., and Ptitsyn, O. B. (1996) Molten globule-like state of cytochrome *c* under conditions simulating those near the membrane surface. *Biochemistry 35*, 6058–6063.
(28) Nishi, K., Komine, Y., Sakai, N., Maruyama, T., and Otagiri, M. (2005) Cooperative effect of hydrophobic and electrostatic forces on alcohol-induced α-helix formation of α_1-acid glycoprotein. *FEBS Lett. 579*, 3596–3600.
(29) Chan, D. C., Chutkowski, C. T., and Kim, P. S. (1998) Evidence that a prominent cavity in the coiled coil of HIV type 1 gp41 is an attractive drug target. *Proc. Natl. Acad. Sci. U.S.A. 95*, 15613–15617.
(30) Liu, S., Jing, W., Cheng, B., Lu, H., Sun, J., Yan, X., Niu, J., Farmar, J., Wu, S., and Jiang, S. (2007) HIV gp41 C-terminal heptad repeat contains multifunctional domains: relation to mechanism of action of anti-HIV peptides. *J. Biol. Chem. 282*, 9612–9620.
(31) Franke, R., Hirsch, T., Overwin, H., and Eichler, J. (2007) Synthetic mimetics of the CD4 binding site of HIV-1 gp120 for the design of immunogens. *Angew. Chem., Int. Ed. 46*, 1253–1255.
(32) Robinson, J. A. (2008) β-hairpin peptidomimetics: design, structures and biological activities. *Acc. Chem. Res. 41*, 1278–1288.
(33) Lu, M., Ji, H., and Shen, S. (1999) Subdomain folding and biological activity of the core structure from human immunodeficiency virus type 1 gp41: implications for viral membrane fusion. *J. Virol. 73*, 4433–4438.
(34) Eckert, D. M., and Kim, P. S. (2001) Design of potent inhibitors of HIV-1 entry from the gp41 N-peptide region. *Proc. Natl. Acad. Sci. U.S.A. 98*, 11187–11192.
(35) Bianchi, E., Finotto, M., Ingallinella, P., Hrin, R., Carella, A. V., Hous, X. S., Schleif, W. A., and Miller, M. D. (2005) Covalent stabilization of coiled coils of the HIV gp41 N region yields extreamely potent and broad inhibitors of viral infection. *Proc. Natl. Acad. Sci. U.S.A. 102*, 12903–12908.
(36) Zwick, M. B., Saphire, E. O., and Burton, D. R. (2004) gp41: HIV's shy protein. *Nat. Med. 10*, 133–134.
(37) Walker, L. M., Phogat, S. K., Chan-Hui, P.-Y., Wagner, D., Phung, P., Goss, J. L., Wrin, T., Simek, M. D., Fling, S., Mitcham, J. L., Lehrman, J. K., Priddy, F. H., Olsen, O. A., Frey, S. M., Hammond, P. W., Kaminsky, S., Zamb, T., Moyle, M., Koff, W. C., Poignard, P., and Burton, D. R. (2009) Broad and potent neutralizing antibodies from an African donor reveal a new HIV-1 vaccine target. *Science 326*, 285–289.

BC900502Z

CHEMMEDCHEM

DOI: 10.1002/cmdc.201000548

Azamacrocyclic Metal Complexes as CXCR4 Antagonists

Tomohiro Tanaka,[a] Tetsuo Narumi,*[a] Taro Ozaki,[a] Akira Sohma,[a] Nami Ohashi,[a] Chie Hashimoto,[a] Kyoko Itotani,[a] Wataru Nomura,[a] Tsutomu Murakami,[b] Naoki Yamamoto,[b, c] and Hirokazu Tamamura*[a]

The chemokine receptor CXCR4 is a member of the seven transmembrane GPCR family, which is implicated in multiple diseases, including HIV infection, cancers, and rheumatoid arthritis. Low-molecular-weight nonpeptidic compounds, including AMD3100 and various pyridyl macrocyclic zinc(II) complexes, have been identified as selective antagonists of CXCR4. In the present study, structure–activity relationship studies were performed by combining the common structural features of alkylamino and pyridiyl macrocyclic antagonists. Several new zinc(II) or copper(II) complexes demonstrated potent anti-HIV activity, strong CXCR4-binding activity, and significant inhibitory activity against Ca^{2+} mobilization induced by CXCL12 stimulation. These results may prove useful in the design of novel CXCR4 antagonists, and the compounds described could potentially be developed as therapeutics against CXCR4-relevant diseases or chemical probes to study the biological activity of CXCR4.

Introduction

The chemokine receptor CXCR4, which transduces signals of its endogenous ligand, CXCL12/stromal cell-derived factor-1 (SDF-1),[1–4] is classified as a member of the seven transmembrane GPCR family, and plays a physiological role via its interaction with CXCL12 in chemotaxis,[5] angiogenesis,[6,7] and neurogenesis[8,9] in embryonic stages. CXCR4 is, however, relevant to multiple diseases including HIV infection/AIDS,[10,11] metastasis of several types of cancer,[12–14] leukemia cell progression,[15,16] and rheumatoid arthritis (RA),[17,18] and is considered an attractive drug target to combat these diseases. Thus, inhibitors targeting CXCR4 are expected to be useful for drug discovery.

Several CXCR4 antagonists have been reported,[19–35] including our discovery of the highly potent CXCR4 antagonist T140, a 14-mer peptide with a disulfide bridge, its smaller derivative, the 5-mer cyclic peptide FC131, and several other potent analogues.[19,24–26,28–30] Clinical development of these peptidic antagonists could be pursued using specific administration strategies involving biodegradable microcapsules.[14,36] However, herein we focus on novel nonpeptidic low-molecular-weight CXCR4 antagonists. To date, AMD3100 (**1**),[20,22] Dpa-Zn complex (**2**),[37] KRH-1636,[27] and other compounds[31–35] have been developed in this and other laboratories as low-molecular-weight nonpeptidic CXCR4 antagonists. The present study reports structure–activity relationship studies based on the combination of common structural motifs, such as xylene scaffolds and cationic moieties that are present in the aforementioned compounds.

Results and Discussion

In order to determine spatially suitable positioning of cationic moieties, *p*- and *m*-xylenes were utilized as spacers. Cationic moieties such as bis(pyridin-2-ylmethyl)amine (dipicolylamine), 1,4,7,10-tetraazacyclododecane (cyclen), and 1,4,8,11-tetraazacyclotetradecane (cyclam) were introduced as R^1 and R^2 (Figure 1). This combination of R^1, R^2, and spacer groups led to the design and synthesis of compounds **12**–**31**.

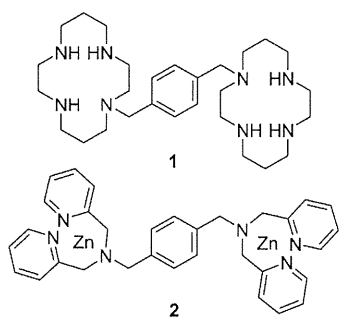

The CXCR4 binding activity of synthetic compounds was assessed based on the inhibition of [^{125}I]CXCL12 binding to Jurkat cells, which express CXCR4.[38] The percent inhibition of all compounds at 1 μM is shown in Table 1. Seven compounds (**16**, **17**, **20**–**22**, **28**, and **29**, Table 1) resulted in greater than 87% inhibition. The high activity of **16** is consistent with re-

[a] T. Tanaka, Dr. T. Narumi, T. Ozaki, A. Sohma, N. Ohashi, C. Hashimoto, K. Itotani, Dr. W. Nomura, Prof. H. Tamamura
Institute of Biomaterials and Bioengineering
Tokyo Medical and Dental University
2-3-10 Kandasurugadai, Chiyoda-ku, Tokyo 101-0062 (Japan)
Fax: (+81) 3-5280-8039
E-mail: tamamura.mr@tmd.ac.jp

[b] Dr. T. Murakami, Prof. N. Yamamoto
AIDS Research Center, National Institute of Infectious Diseases
1-23-1 Toyama, Shinjuku-ku, Tokyo 162-8640 (Japan)

[c] Prof. N. Yamamoto
Department of Microbiology, Yong Loo Lin School of Medicine
National University of Singapore, Singapore 117597 (Singapore)

Supporting information for this article is available on the WWW under http://dx.doi.org/10.1002/cmdc.201000548.

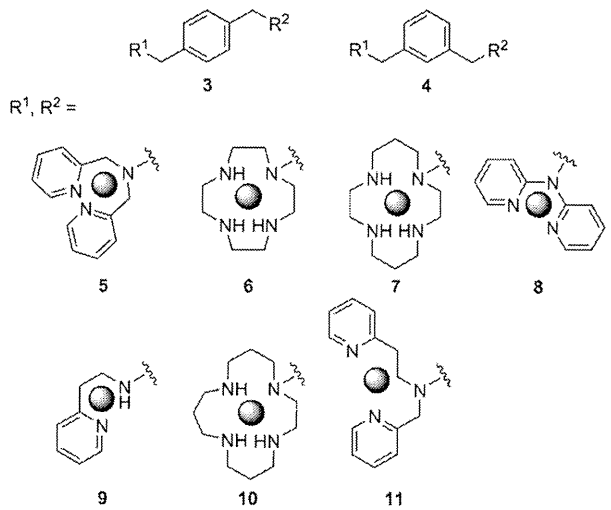

Figure 1. The structures of aromatic spacers (upper) and cationic moieties (R^1 and R^2). The shaded circle represents the position of the metal cation (Zn^{II} or Cu^{II}) in the chelate.

sults reported previously.[20,22] The anti-HIV activities of **17** and **29**, which contain only cyclam or cyclal rings, were reported by De Clercq et al.[39,40] Compounds with only pyridine and/or cyclen rings did not show any high binding activity. The presence of azamacrocyclic rings is presumably indispensable to the interaction of these compounds with CXCR4, and the size of rings appears to be important because not only compounds **16** and **17**, with two cyclam rings in the molecule, but also compounds **28** and **29**, with two cyclal rings, have remarkably more potent CXCR4 binding activity than compounds **14** and **15**, which have two cyclen rings. Compound **22**, with a *p*-xylene moiety, exhibited higher activity than compound **23**, which has an *m*-xylene moiety, indicating that *p*-xylene is more suitable than *m*-xylene as a spacer for approximate positioning of cationic moieties. At 0.1 μM, compound **22** resulted in 86% inhibition of [^{125}I]CXCL12 binding, while the other six compounds exhibited 37–66% inhibition. The IC_{50} value of compound **22** was estimated to be 37 nM.

$ZnCl_2$ was added to phosphate-buffered saline (PBS) solutions of these 20 compounds, **12–31**, to form zinc(II) complexes. The percent inhibition for each compound at 1 μM against [^{125}I]CXCL12 binding was determined and is given in Table 1. Zinc complexation of **12–15**, **18**, **19**, and **23** resulted in a remarkable increase in CXCR4 binding activity compared to the corresponding zinc-free compounds. These molecules contain dipicolylamine and/or cyclen moieties, suggesting that chelation of the nitrogen atoms with the zinc(II) ion significantly affects their interactions with CXCR4. The high activity of the zinc chelates of **12** and **13** is consistent with results provided in our previous paper.[37] Additionally, the anti-HIV activity of zinc complexes of **14** and **15** was reported by Kimura et al.[41] For compounds with only dipicolylamine and/or cyclen macrocycles as cationic moieties (**12–15**, **18**, and **19**), zinc complexation is critical to achieve high binding activity; the corresponding zinc-free compounds exhibit no significant activity. Compounds **16**, **17**, **20–22**, **28**, and **29** demonstrated high binding affinity in metal-free states as well as in zinc complexation states, indicating that zinc complexation of either of the macrocyclic rings in these compounds is not essential for high activity. The CXCR4 binding activity and anti-HIV activity of the zinc complex of **16** were reported previously.[42,43] Measured inhibition percentages for 0.1 μM of the zinc complexes of **12**, **14–23**, **28**, and **29** are given in Table 1. The zinc complexes of **20–22**, **28**, and **29** at 0.1 μM exhibited greater than 79% inhibition of [^{125}I]CXCL12 binding, and the other eight zinc complexes (of **12**, **14–19**, and **23**,) showed less than 55% inhibition. The IC_{50} values of zinc complexes of **20–22**, **28**, and **29** were estimated to be 11, 8.3, 22, 40, and 52 nM, respectively. Zinc complexes of compounds containing a combination of cyclen and cyclam moieties, **20** and **21**, had remarkably potent IC_{50} values.

To form chelates with a copper(II) cation, $CuCl_2$ was added to solutions in PBS of **12-31**. The inhibition percentages of all the compounds at 1 μM against [^{125}I]CXCL12 binding are shown in Table 1. Copper complexes of **14** and **15** exhibited a significant increase in CXCR4 binding activity as compared to the corresponding copper-free compounds, a phenomenon which is also seen in the zinc chelates. These compounds have two cyclen moieties in the molecules, suggesting that zinc or copper complexation is critical for high binding activity. Compounds **16**, **17**, and **20–22** showed high binding affinities in metal-free states and zinc- and copper-complexed states, indicating that metallic complexation of the cyclam rings in these compounds is not necessary for high activity. The CXCR4 binding activity of the copper complex of **16** was previously reported.[42] For compounds **17**, **22**, **23**, **28**, and **29**, copper complexation caused a significant decrease in binding activity compared to the corresponding copper-free compounds, whereas for compounds **14**, **15**, **18**, and **19**, copper complexation caused an increase in binding activity. This phenomenon may be due to the difference in ring sizes and structures of macrocycles, and was not observed upon zinc-complex formation. Inhibition at 0.1 μM of the copper complexes of **16** and **20–22**, which exhibited greater than 85% inhibition of [^{125}I]CXCL12 binding at 1 μM, are given in Table 1. The copper complexes of **16**, **20**, **21**, and **22** at 0.1 μM showed 39, 69, 88, and 39% inhibition, respectively, with the IC_{50} value of the copper complex of **21** estimated to be 16 nM.

Molecular modeling analysis of compound **21** and its zinc(II) and copper(II) complexes predicted that these complexes would form a stable coordinate conformation as shown in Figure 2. In general, zinc(II) complexes are predicted to adopt a tetrahedral conformation, while copper(II) complexes form a planar four coordinate/square conformation. The zinc(II) complex of **21** is predicted to have a tetrahedral conformation and the copper(II) complex a square planar conformation in both the cyclen and cyclam rings. The carboxyl group of either Asp 171 or Asp 262 in CXCR4 is thought to coordinate strongly with zinc ions but not copper ions in the complexes,[41–43] and as a consequence, the zinc complex of **21** would bind more strongly than **21** or its copper complex. This order of binding

Table 1. CXCR4 binding activity of compounds **12–31** in the metal ion-free form, the zinc complex, and the copper complex.

Compd	Spacer	R^1	R^2	Metal free			Zinc complex			Copper complex		
				Inhibition[a] [%]		IC_{50}[b]	Inhibition[a] [%]		IC_{50}[b]	Inhibition[a] [%]		IC_{50}[b]
				1 μM	0.1 μM	[nM]	1 μM	0.1 μM	[nM]	1 μM	0.1 μM	[nM]
12	*p*-xylene	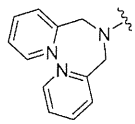	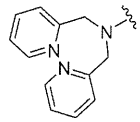	0	n.d.	n.d.	83±2	24±5	n.d.	10±4	n.d.	n.d.
13	*m*-xylene			0	n.d.	n.d.	31±3	n.d.	n.d.	0	n.d.	n.d.
14	*p*-xylene	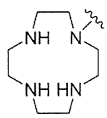	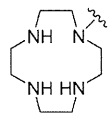	30±4	n.d.	n.d.	87±4	0	n.d.	60±2	n.d.	n.d.
15	*m*-xylene			33±2	n.d.	n.d.	94±1	13±6	n.d.	80±3	n.d.	n.d.
16	*p*-xylene	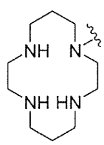	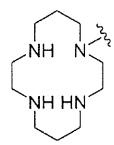	94±4	59±6	n.d.	97±5	28±3	n.d.	98±1	39±3	n.d.
17	*m*-xylene			95±3	49±9	n.d.	98±4	55±7	n.d.	75±1	n.d.	n.d.
18	*p*-xylene	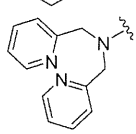	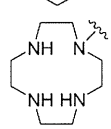	32±0.7	n.d.	n.d.	97±6	0	n.d.	52±3	n.d.	n.d.
19	*m*-xylene			17±5	n.d.	n.d.	91±4	0	n.d.	22±6	n.d.	n.d.
20	*p*-xylene	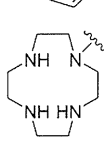	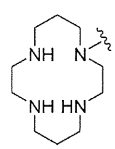	89±3	62±3	n.d.	>100	79±1	11	>100	69±3	n.d.
21	*m*-xylene			89±3	66±3	n.d.	92±3	>100	8.3	>100	88±1	16
22	*p*-xylene	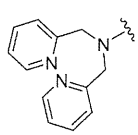	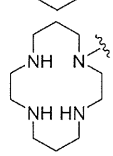	94±3	86±3	37	99±8	79±0.6	22	85±3	39±3	n.d.
23	*m*-xylene			58±8	n.d.	n.d.	90±17	37±0.3	n.d.	48±4	n.d.	n.d.
24	*p*-xylene	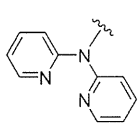	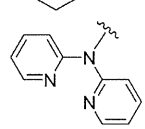	3±0.9	n.d.	n.d.	0	n.d.	n.d.	0	n.d.	n.d.
25	*m*-xylene			4±3	n.d.	n.d.	0	n.d.	n.d.	0	n.d.	n.d.
26	*p*-xylene	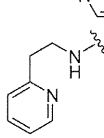	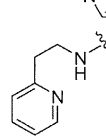	14±2	n.d.	n.d.	10±3	n.d.	n.d.	0	n.d.	n.d.
27	*m*-xylene			10±3	n.d.	n.d.	10±4	n.d.	n.d.	0	n.d.	n.d.
28	*p*-xylene	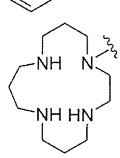	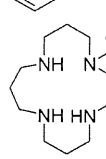	91±0.4	37±0.9	n.d.	97±4	>100	40	57±4	n.d.	n.d.
29	*m*-xylene			87±2	50±1	n.d.	>100	91±4	52	55±1	n.d.	n.d.
30	*p*-xylene	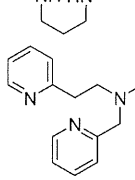	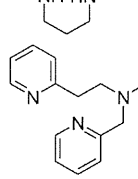	0	n.d.	n.d.	14±3	n.d.	n.d.	14±3	n.d.	n.d.
31	*m*-xylene			24±2	n.d.	n.d.	20±3	n.d.	n.d.	0	n.d.	n.d.
FC-131	*cyclo*-[D-Tyr-Arg-Arg-Nal-Gly-]			100	100	1.8	–	–	–	–	–	–

[a] CXCR4 binding activity was assessed based on inhibition of [^{125}I]CXCL12 binding to Jurkat cells. Percent inhibition for all compounds at 1 and 0.1 μM were calculated relative to the percent inhibition by FC131 (100%). [b] IC_{50} values are the concentrations which correspond to 50% inhibition of [^{125}I]CXCL12 binding to Jurkat cells. All data are mean values ±SEM of at least three independent experiments. n.d. = not determined.

affinities is commonly seen for these compounds and their zinc(II) or copper(II) complexes.

We investigated the CXCR4 antagonistic activity of compound **22** and the zinc complexes of **20**, **21**, **22**, and **28**, all of which possess strong CXCR4 binding activity. The CXCR4 antagonistic activity was assessed based on the inhibitory activity of the compounds against Ca^{2+} mobilization induced by CXCL12 stimulation through CXCR4 (figure S1 in the Support-

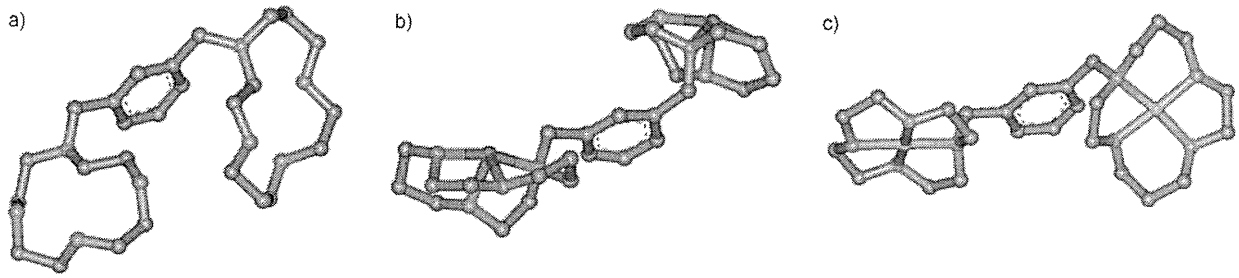

Figure 2. Structures calculated by molecular modeling of a) compound **21**, and its b) zinc and c) copper complexes. Atom color code: nitrogen = blue, carbon = gray, zinc = red, copper = light red.

ing Information). All of the tested compounds showed significant antagonistic activity at 1 μM.

The representative compounds **14**, **16**, **20**–**23**, **28**, and **29**, as well as their zinc chelates, were evaluated for anti-HIV activity. CXCR4 is the major co-receptor for the entry of T-cell-line-tropic (X4) HIV-1.[10,11] Inhibitory activity against X4-HIV-1 (NL4-3 strain)-induced cytopathogenicity in MT-4 cells was assessed and is shown in Table 2.[38] A correlation between CXCR4 binding activity and anti-HIV activity was observed. For compound **16** and its zinc complex, anti-HIV activity was significantly stronger than CXCR4 binding activity, and for the zinc complexes of compounds **20**–**22**, the CXCR4 binding activity is two to four-times stronger than the anti-HIV activity. The anti-HIV activity of the zinc complex of **16** was the most potent (EC_{50} = 8.2 nM). This is comparable to the anti-HIV activities of **16** and its zinc complex that were reported previously.[20,22,42,43] The zinc complex of **21**, which was the most active compound in terms of CXCR4 binding activity, also exhibited potent anti-HIV activity (EC_{50} = 36 nM).

Taken together, these results show that all of the compounds exhibiting CXCR4 binding activity also showed significant anti-HIV activity (EC_{50} values < 300 nM), and none of the tested compounds exhibited significant cytotoxicity (CC_{50} values > 10 μM; Table 2). Conversely, zinc complexes of **20**, **21**, **22**, and **28** did not exhibit significant anti-HIV activity against macrophage-tropic (R5) HIV-1 (NL(AD8) strain)-induced cytopathogenicity in PM-1 cells at concentrations below 10 μM. Since R5-HIV-1 strains use CCR5 instead of CXCR4 as the major co-receptor for entry, this suggests that these compounds do not bind CCR5 but rather are highly selective for CXCR4.

Table 2. Anti-HIV activity and cytotoxicity of representative compounds in the metal ion-free and zinc chelates.

Compd	Metal ion-free		Zinc chelate	
	EC_{50}[a] [nM]	CC_{50}[b] [μM]	EC_{50}[a] [nM]	CC_{50}[b] [μM]
14	200	> 10	200	> 10
16	21	> 10	8.2	> 10
20	38	> 10	39	> 10
21	50	> 10	36	> 10
22	93	> 10	48	> 10
23	290	> 10	220	> 10
28	36	> 10	56	> 10
29	130	> 10	42	> 10
FC131	93	> 10		
AZT	69	> 100		

[a] EC_{50} values are the concentrations corresponding to 50% protection from X4-HIV-1 (NL4–3 strain)-induced cytopathogenicity in MT-4 cells. [b] CC_{50} values are the concentrations at which the viability of MT-4 cells is reduced by 50%. All data are mean values from at least three independent experiments.

Conclusions

The present study introduces a new class of low-molecular-weight CXCR4 antagonists and their zinc(II) or copper(II) complexes, which contain pyridyl or azamacrocycle moieties with *p*-xylene or *m*-xylene spacers. These compounds demonstrated strong CXCR4 binding activity. Zinc complexes of **20** and **21**, which were the two most active compounds, contain cyclen and cyclam rings with *p*- and *m*-xylene spacers and exhibited remarkably potent IC_{50} values (11 and 8.3 nM, respectively). These compounds showed significant CXCR4 antagonistic activity, based on inhibitory activity against Ca^{2+} mobilization induced by CXCL12 stimulation through CXCR4, as well as potent anti-HIV activity, as assessed by protection from X4-HIV-1-induced cytopathogenicity in MT-4 cells. These results provide useful insights into the future design of novel CXCR4 antagonists, complementing information from other CXCR4 antagonists such as T140, FC131, and KRH-1636. Furthermore, these new compounds are useful for the development of therapeutic strategies for CXCR4-relevant diseases and chemical probes to study the biological activity of CXCR4.

Experimental Section

Chemistry

Compounds **12**–**17**, **20**, **21**, **24**, **25**, **27**–**29**, and **31** were synthesized as previously reported.[20,22,37,40,41,44–47] Compounds **18**, **19**, **22**, **23**, **26**, and **30** were synthesized in the present study; details are provided in the Supporting Information. A representative compound, **18**, was synthesized by coupling *p*-dibromoxylene (1,4-bis-(bromomethyl)benzene) with tri-Boc-protected 1,4,7,10-tetraazacyclododecane, followed by treatment with trifluoroacetic acid and subsequent coupling with bis(pyridin-2-ylmethyl)amine. All crude compounds were purified by RP-HPLC and identified by FAB/ESI-

HRMS. Zinc(II) or copper(II) complex formation was accomplished by treatment of the above compounds with 10 equiv of $ZnCl_2$ or $CuCl_2$ in PBS. All zinc(II) or copper(II) complexes were characterized by chemical shifts of their methylene protons in ^1H NMR analysis. The pyridyl zinc(II) complex was characterized previously,[37] and zinc(II) or copper(II) complex formation with these macrocyclic compounds has been reported elsewhere.[41,42,48,49] Detailed procedures and data are provided in the Supporting Information.

Biological assays

A CXCR4 binding assay for compounds, based on the inhibition of [^{125}I]CXCL12 binding to Jurkat cells, was performed as reported by Tanaka et al.[38] CXCR4 antagonistic activity was evaluated as described by Ichiyama et al[27], measuring inhibitory activity against Ca^{2+} mobilization induced by CXCL12 stimulation in HOS cells expressing CXCR4. Anti-HIV activity was determined by inhibitory activity against X4-HIV-1(NL4–3)-induced cytopathogenicity in MT-4 cells as reported by Tanaka et al.[38] An X4 HIV-1 infectious molecular clone (pNL4–3) was obtained from the AIDS Research and Reference Reagent Program. The virus NL4–3 was obtained from the culture supernatant of 293T cells transfected with pNL4–3.

Molecular modeling

Molecular modeling calculations were performed using Sybyl (version 7.0, Tripos). Energy minimization was performed using the Tripos force field and Gasteiger–Hückel charge parameters. The lowest energy conformation was obtained by random search methods.

Acknowledgements

T.T. and N.O. are supported by research fellowships for young scientists from the Japan Society for the Promotion of Science. This work was supported in part by a Grant-in-Aid for Scientific Research from the Ministry of Education, Culture, Sports, Science, and Technology of Japan, and Health and Labor Sciences Research Grants from the Japanese Ministry of Health, Labor, and Welfare. The authors thank Mr. Wu Honggui (Tokyo University of Science) for his assistance with the anti-HIV assay.

Keywords: azamacrocycles · Ca^{2+} mobilization · CXCR4 · HIV · structure–activity relationships

[1] T. Nagasawa, H. Kikutani, T. Kishimoto, *Proc. Natl. Acad. Sci. USA* **1994**, *91*, 2305–2309.
[2] C. C. Bleul, M. Farzan, H. Choe, C. Parolin, I. Clark-Lewis, J. Sodroski, T. A. Springer, *Nature* **1996**, *382*, 829–833.
[3] E. Oberlin, A. Amara, F. Bachelerie, C. Bessia, J. L. Virelizier, F. Arenzana-Seisdedos, O. Schwartz, J. M. Heard, I. Clark-Lewis, D. L. Legler, M. Loetscher, M. Baggiolini, B. Moser, *Nature* **1996**, *382*, 833–835.
[4] K. Tashiro, H. Tada, R. Heilker, M. Shirozu, T. Nakano, T. Honjo, *Science* **1993**, *261*, 600–603.
[5] C. C. Bleul, R. C. Fuhlbrigge, J. M. Casanovas, A. Aiuti, T. A. Springer, *J. Exp. Med.* **1996**, *184*, 1101–1109.
[6] K. Tachibana, S. Hirota, H. Iizasa, H. Yoshida, K. Kawabata, Y. Kataoka, Y. Kitamura, K. Matsushima, N. Yoshida, S. Nishikawa, T. Kishimoto, T. Nagasawa, *Nature* **1998**, *393*, 591–594.
[7] T. Nagasawa, S. Hirota, K. Tachibana, N. Takakura, S. Nishikawa, Y. Kitamura, N. Yoshida, H. Kikutani, T. Kishimoto, *Nature* **1996**, *382*, 635–638.
[8] Y. Zhu, Y. Yu, X. C. Zhang, T. Nagasawa, J. Y. Wu, Y. Rao, *Nat. Neurosci.* **2002**, *5*, 719–720.
[9] R. K. Stumm, C. Zhou, T. Ara, F. Lazarini, M. Dubois-Dalcq, T. Nagasawa, V. Hollt, S. Schulz, *J. Neurosci.* **2003**, *23*, 5123–5130.
[10] H. K. Deng, R. Liu, W. Ellmeier, S. Choe, D. Unutmaz, M. Burkhart, P. D. Marzio, S. Marmon, R. E. Sutton, C. M. Hill, C. B. Davis, S. C. Peiper, T. J. Schall, D. R. Littman, N. R. Landau, *Nature* **1996**, *381*, 661–666.
[11] Y. Feng, C. C. Broder, P. E. Kennedy, E. A. Berger, *Science* **1996**, *272*, 872–877.
[12] T. Koshiba, R. Hosotani, Y. Miyamoto, J. Ida, S. Tsuji, S. Nakajima, M. Kawaguchi, H. Kobayashi, R. Doi, T. Hori, N. Fujii, M. Imamura, *Clin. Cancer Res.* **2000**, *6*, 3530–3535.
[13] A. Müller, B. Homey, H. Soto, N. Ge, D. Catron, M. E. Buchanan, T. McClanahan, E. Murphy, W. Yuan, S. N. Wagner, J. L. Barrera, A. Mohar, E. Verastegui, A. Zlotnik, *Nature* **2001**, *410*, 50–56.
[14] H. Tamamura, A. Hori, N. Kanzaki, K. Hiramatsu, M. Mizumoto, H. Nakashima, N. Yamamoto, A. Otaka, N. Fujii, *FEBS Lett.* **2003**, *550*, 79–83.
[15] N. Tsukada, J. A. Burger, N. J. Zvaifler, T. J. Kipps, *Blood* **2002**, *99*, 1030–1037.
[16] J. Juarez, K. F. Bradstock, D. J. Gottlieb, L. J. Bendall, *Leukemia* **2003**, *17*, 1294–1300.
[17] T. Nanki, K. Hayashida, H. S. El-Gabalawy, S. Suson, K. Shi, H. J. Girschick, S. Yavuz, P. E. Lipsky, *J. Immunol.* **2000**, *165*, 6590–6598.
[18] H. Tamamura, M. Fujisawa, K. Hiramatsu, M. Mizumoto, H. Nakashima, N. Yamamoto, A. Otaka, N. Fujii, *FEBS Lett.* **2004**, *569*, 99–104.
[19] T. Murakami, T. Nakajima, Y. Koyanagi, K. Tachibana, N. Fujii, H. Tamamura, N. Toshida, M. Waki, A. Matsumoto, O. Yoshie, T. Kishimoto, N. Yamamoto, T. Nagasawa, *J. Exp. Med.* **1997**, *186*, 1389–1393.
[20] D. Schols, S. Struyf, J. Van Damme, J. A. Este, G. Henson, E. DeClarcq, *J. Exp. Med.* **1997**, *186*, 1383–1388.
[21] B. J. Doranz, K. Grovit-Ferbas, M. P. Sharron, S.-H. Mao, M. Bidwell Goetz, E. S. Daar, R. W. Doms, W. A. O'Brien, *J. Exp. Med.* **1997**, *186*, 1395–1400.
[22] G. A. Donzella, D. Schols, S. W. Lin, J. A. Este, K. A. Nagashima, *Nat. Med.* **1998**, *4*, 72–76.
[23] O. M. Z. Howard, J. J. Oppenheim, M. G. Hollingshead, J. M. Covey, J. Bigelow, J. J. McCormack, R. W. Buckheit, Jr., D. J. Clanton, J. A. Turpin, W. G. Rice, *J. Med. Chem.* **1998**, *41*, 2184–2193.
[24] H. Tamamura, Y. Xu, T. Hattori, X. Zhang, R. Arakaki, K. Kanbara, A. Omagari, A. Otaka, T. Ibuka, N. Yamamoto, H. Nakashima, N. Fujii, *Biochem. Biophys. Res. Commun.* **1998**, *253*, 877–882.
[25] H. Tamamura, A. Omagari, S. Oishi, T. Kanamoto, N. Yamamoto, S. C. Peiper, H. Nakashima, A. Otaka, N. Fujii, *Bioorg. Med. Chem. Lett.* **2000**, *10*, 2633–2637.
[26] N. Fujii, S. Oishi, K. Hiramatsu, T. Araki, S. Ueda, H. Tamamura, A. Otaka, S. Kusano, S. Terakubo, H. Nakashima, J. A. Broach, J. O. Trent, Z. Wang, S. C. Peiper, *Angew. Chem.* **2003**, *115*, 3373–3375; *Angew. Chem. Int. Ed.* **2003**, *42*, 3251–3253.
[27] K. Ichiyama, S. Yokoyama-Kumakura, Y. Tanaka, R. Tanaka, K. Hirose, K. Bannai, T. Edamatsu, M. Yanaka, Y. Niitani, N. Miyano-Kurosaki, H. Takaku, Y. Koyanagi, N. Yamamoto, *Proc. Natl. Acad. Sci. USA* **2003**, *100*, 4185–4190.
[28] H. Tamamura, N. Fujii, *Curr. Drug Targets-Infectious Disorders* **2004**, *4*, 103–110.
[29] H. Tamamura, K. Hiramatsu, S. Ueda, Z. Wang, S. Kusano, S. Terakubo, J. O. Trent, S. C. Peiper, N. Yamamoto, H. Nakashima, A. Otaka, N. Fujii, *J. Med. Chem.* **2005**, *48*, 380–391.
[30] H. Tamamura, T. Araki, S. Ueda, Z. Wang, S. Oishi, A. Esaka, J. O. Trent, H. Nakashima, N. Yamamoto, S. C. Peiper, A. Otaka, N. Fujii, *J. Med. Chem.* **2005**, *48*, 3280–3289.
[31] G. C. Valks, G. McRobbie, E. A. Lewis, T. J. Hubin, T. M. Hunter, P. J. Sadler, C. Pannecouque, E. De Clercq, S. J. Archibald, *J. Med. Chem.* **2006**, *49*, 6162–6165.
[32] W. Zhan, Z. Liang, A. Zhu, S. Kurtkaya, H. Shim, J. P. Snyder, D. C. Liotta, *J. Med. Chem.* **2007**, *50*, 5655–5664.
[33] A. Khan, G. Nicholson, J. Greenman, L. Madden, G. McRobbie, C. Pannecouque, E. De Clercq, R. Ullom, D. L. Maples, R. D. Maples, J. D. Silversides, T. J. Hubin, S. J. Archibald, *J. Am. Chem. Soc.* **2009**, *131*, 3416–3417.
[34] G. J. Bridger, R. T. Skerlj, P. E. Hernandez-Abad, D. E. Bogucki, Z. Wang, Y. Zhou, S. Nan, E. M. Boehringer, T. Wilson, J. Crawford, M. Metz, S. Hatse, K. Princen, E. De Clercq, D. Schols, *J. Med. Chem.* **2010**, *53*, 1250–1260.

[35] R. T. Skerlj, G. J. Bridger, A. Kaller, E. J. McEachern, J. B. Crawford, Y. Zhou, B. Atsma, J. Langille, S. Nan, D. Veale, T. Wilson, C. Harwig, S. Hatse, K. Princen, E. De Clercq, D. Schols, *J. Med. Chem.* **2010**, *53*, 3376–3388.
[36] M. Takenaga, H. Tamamura, K. Hiramatsu, N. Nakamura, Y. Yamaguchi, A. Kitagawa, S. Kawai, H. Nakashima, N. Fujii, R. Igarashi, *Biochem. Biophys. Res. Commun.* **2004**, *320*, 226–232.
[37] H. Tamamura, A. Ojida, T. Ogawa, H. Tsutsumi, H. Masuno, H. Nakashima, N. Yamamoto, I. Hamachi, N. Fujii, *J. Med. Chem.* **2006**, *49*, 3412–3415.
[38] T. Tanaka, H. Tsutsumi, W. Nomura, Y. Tanabe, N. Ohashi, A. Esaka, C. Ochiai, J. Sato, K. Itotani, T. Murakami, K. Ohba, N. Yamamoto, N. Fujii, H. Tamamura, *Org. Biomol. Chem.* **2008**, *6*, 4374–4377.
[39] G. J. Bridger, R. T. Skerlj, D. Thornton, S. Padmanabhan, S. A. Martellucci, G. W. Henson, M. J. Abrams, N. Yamamoto, K. De Vreese, R. Pauwels, E. De Clercq, *J. Med. Chem.* **1995**, *38*, 366–378.
[40] G. J. Bridger, R. T. Skerlj, S. Padmanabhan, S. A. Martellucci, G. W. Henson, M. J. Abrams, H. C. Joao, M. Witvrouw, K. De Vreese, R. Pauwels, E. De Clercq, *J. Med. Chem.* **1996**, *39*, 109–119.
[41] Y. Inouye, T. Kanamori, T. Yoshida, T. Koike, M. Shionoya, H. Fujioka, E. Kimura, *Biol. Pharm. Bull.* **1996**, *19*, 456–458.
[42] L. O. Gerlach, J. S. Jakobsen, K. P. Jensen, M. R. Rosenkilde, R. T. Skerlj, U. Ryde, G. J. Bridger, T. W. Schwartz, *Biochemistry* **2003**, *42*, 710–717.
[43] H. F. Egberink, E. De Clercq, A. L. Van Vliet, J. Balzarini, G. J. Bridger, G. Henson, M. C. Horzinek, D. Schols, *J. Virol.* **1999**, *73*, 6346–6352.
[44] M. Le Baccon, F. Chuburu, L. Toupet, H. Handel, M. Soibinet, I. Dechamps-Olivier, J.-P. Barbier, M. Aplincourt, *New J. Chem.* **2001**, *25*, 1168–1174.
[45] B. Antonioli, D. J. Bray, J. K. Clegg, K. Gloe, K. Gloe, O. Kataeva, L. F. Lindoy, J. C. McMurtrie, P. J. Steel, C. J. Sumby, M. Wenzel, *Dalton Trans.* **2006**, 4783–4794.
[46] S. P. Foxon, D. Utz, J. Astner, S. Schindler, F. Thaler, F. W. Heinemann, G. Liehr, J. Mukherjee, V. Balamurugan, D. Ghosh, R. Mukherjee, *Dalton Trans.* **2004**, 2321–2328.
[47] S. Mandal, F. Lloret, R. Mukherjee, *Inorg. Chim. Acta* **2009**, *362*, 27–37.
[48] M. Soibinet, I. De'champs-Olivier, E. Guillon, J.-P. Barbier, M. Aplincourt, F. Chuburu, M. Le Baccon, H. Handel, *Eur. J. Inorg. Chem.* **2003**, 1984–1994.
[49] R. W. Hay, M. T. Tarafder, *Transition Met. Chem.* **1990**, *15*, 490–492.

Received: December 19, 2010
Published online on February 10, 2011

Bioorganic & Medicinal Chemistry 20 (2012) 1468–1474

Contents lists available at SciVerse ScienceDirect

Bioorganic & Medicinal Chemistry

journal homepage: www.elsevier.com/locate/bmc

Conjugation of cell-penetrating peptides leads to identification of anti-HIV peptides from matrix proteins

Tetsuo Narumi [a], Mao Komoriya [a], Chie Hashimoto [a], Honggui Wu [b,c], Wataru Nomura [a], Shintaro Suzuki [a], Tomohiro Tanaka [a], Joe Chiba [c], Naoki Yamamoto [d], Tsutomu Murakami [b,*], Hirokazu Tamamura [a,*]

[a] Institute of Biomaterials and Bioengineering, Tokyo Medical and Dental University, Chiyoda-ku, Tokyo 101-0062, Japan
[b] AIDS Research Center, National Institute of Infectious Diseases, Shinjuku-ku, Tokyo 162-8640, Japan
[c] Department of Biological Science Technology, Tokyo University of Science, Noda, Chiba 278-8510, Japan
[d] Yong Loo Lin School of Medicine, National University of Singapore, Singapore 117597, Singapore

ARTICLE INFO

Article history:
Received 6 December 2011
Revised 24 December 2011
Accepted 24 December 2011
Available online 2 January 2012

Keywords:
Matrix protein
Octa-arginyl group
Overlapping peptide
Anti-HIV

ABSTRACT

Compounds which inhibit the HIV-1 replication cycle have been found amongst fragment peptides derived from an HIV-1 matrix (MA) protein. Overlapping peptide libraries covering the whole sequence of MA were designed and constructed with the addition of an octa-arginyl group to increase their cell membrane permeability. Imaging experiments with fluorescent-labeled peptides demonstrated these peptides with an octa-arginyl group can penetrate cell membranes. The fusion of an octa-arginyl group was proven to be an efficient way to find active peptides in cells such as HIV-inhibitory peptides.

1. Introduction

Several anti-retroviral drugs beyond reverse transcriptase inhibitors, including effective protease inhibitors[1] and integrase inhibitors[2,3] are currently available to treat human immunodeficiency virus type 1 (HIV-1) infected individuals. We have also developed several anti-HIV agents such as coreceptor CXCR4 antagonists,[4–7] CD4 mimics,[8–10] fusion inhibitors[11] and integrase inhibitors.[12,13] However, the emergence of viral strains with multi-drug resistance (MDR), which accompanies the development of any antiviral drug, has encouraged a search for new types of anti-HIV-1 drugs with different inhibitory mechanisms.

Matrix (MA) proteins are essential for assembly of the virion shell. MA is a component of the Gag precursor protein, Pr55Gag, and is located within the viral membrane.[14,15] It has been reported that MA-derived peptides such as MA(47–59) inhibit infection by HIV,[16] and that MA-derived peptides such as MA(31–45) and MA(41–55) show anti-HIV activity.[17] In addition, Morikawa et al. report that MA(61–75) and MA(71–85) inhibit MA dimerization, a necessary step in the formation of the virion shell.[18] However, the question of whether the above MA peptides can penetrate cell membranes was not addressed in these reports. We speculate that to achieve antiviral activity it is essential that the MA-derived peptides penetrate the cell membrane and function intracellularly. In this paper, we report our design and construction of an overlapping library of fragment peptides derived from the MA protein with a cell membrane permeable signal. Our aim is the discovery of potent lead compounds, which demonstrate HIV inhibitory activity inside the host cells.

2. Materials and methods

2.1. Peptide synthesis

MA-derived fragments and an octa-arginyl (R_8) peptide were synthesized by stepwise elongation techniques of Fmoc-protected amino acids on a Rink amide resin. Coupling reactions were performed using 5.0 equiv of Fmoc-protected amino acid, 5.0 equiv of diisopropylcarbodiimide and 5.0 equiv of 1-hydroxybenzotriazole monohydrate. Ac_2O–pyridine (1/1, v/v) for 20 min was used to acetylate the N-terminus of MA-derived fragments, with the exception of fragment 1. Chloroactylation of the N-terminus of the R_8 peptide, was achieved with 40 equiv of chloroacetic acid, 40 equiv of diisopropylcarbodiimide and 40 equiv of 1-hydroxybenzotriazole monohydrate, treated for 1 h. Cleavage of peptides from resin and side chain deprotection were carried out by stirring for 1.5 h with a mixture of TFA, thioanisole, ethanedithiol, *m*-cresol

* Corresponding authors. Tel.: +81 3 5285 1111; fax: +81 3 5285 5037 (T.M.); tel.: +81 3 5280 8036; fax: +81 3 5280 8039 (H.M.).
E-mail addresses: tmura@nih.go.jp (T. Murakami), tamamura.mr@tmd.ac.jp (H. Tamamura).

0968-0896/$ - see front matter © 2011 Elsevier Ltd. All rights reserved.
doi:10.1016/j.bmc.2011.12.055

and triisopropylsilane (8.15/0.75/0.75/0.25/0.25/0.1, v/v). After removal of the resins by filtration, the filtrate was concentrated under reduced pressure, and crude peptides were precipitated in cooled diethyl ether. All crude peptides were purified by RP-HPLC and identified by ESI-TOFMS. In the conjugation of the R_8 peptide (or iodoacetamide), the peptide (or iodoacetamide) solution in 0.1 M phosphate buffer, pH 7.8 was added to MA fragments which were synthesized as described above. The reaction mixture was stirred at room temperature under nitrogen. After 24 h (or 1 h for the conjugation of iodoacetamide), purification was performed by RP-HPLC. The purified peptides were identified by ESI-TOF MS and lyophilized. Purities of all final compounds were confirmed to be >95% by analytical HPLC. Detailed data are provided in Supplementary data.

2.2. Anti-HIV-1 assay

Anti-HIV-1 (NL4-3 or NL(AD8)) activity was determined by measurement of the protection against HIV-1-induced cytopathogenicity in MT-4 cells or PM1/CCR5 cells. Various concentrations of test peptide solutions were added to HIV-1 infected MT-4 or PM1/CCR5 cells at multiplicity of infection (MOI) of 0.001 and placed in wells of a 96-well microplate. After 5 day incubation at 37 °C in a CO_2 incubator, the number of viable cells was determined using the 3-(4,5-dimethylthiazol-2-yl)-2,5-diphenyltetrazolium bromide (MTT) method. The anti-HIV-1 (JR-CSF) activity was also determined by measuring capsid p24 antigen concentrations of the culture supernatant in the infected cultures by a commercially available ELISA assay (ZeptoMetrix Corp., Buffalo, NY).

2.3. CD spectroscopy

CD spectra were recorded on a JASCO J-720 spectropolarimeter at 25 °C. The measurements were performed using a 0.1 cm path length cuvette at a 0.1 nm spectral resolution. Each spectrum represents the average of 10 scans, and the scan rate was 50 nm/min. The concentrations of samples 8L and 9L were 28.2 and 64.7 μM, respectively, in PBS buffer (pH 7.4).

2.4. Fluorescent imaging of cell-penetrating MA peptides

Cells were seeded on 35 mm glass-bottom dish (2×10^5 cells/dish for HeLa and A549, 1×10^5 cells/dish for CHO-K1) one day before the experiments. The cells were cultured in DMEM/10% FBS/Penicillin–Streptomycin for HeLa and A549, or Ham's F12/10% FBS/Penicillin–Streptomycin for CHO-K1 at 37 °C/5% CO_2. Before the addition of MA peptides, cells were washed with Hanks' balanced salt solutions (HBSS) once. Peptides were added at 5 μM and further cultured for 30 min at 37 °C/5% CO_2. After incubation, cells were washed three times with HBSS and observed under a confocal laser-scanning microscopy (Zeiss LSM510).

3. Results and discussion

An overlapping peptide library spanning the whole sequence of the MA domain, p17, of NL4-3, the Gag precursor Pr55 of HIV-1 was designed. The full sequence of MA consists of 132 amino acid residues. In the peptide library, the MA sequence was divided from the N-terminus in 15-residue segments with an overlap of 5

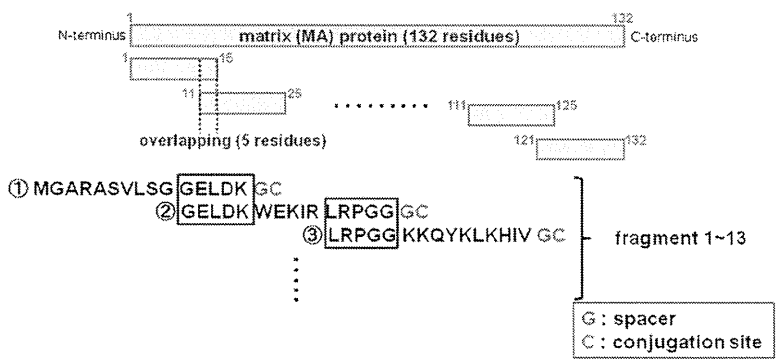

fragment number	sequence
1	H-MGARASVLSGGELDKGC-NH_2
2	CH_3CO-GELDKWEKIRLRPGGGC-NH_2
3	CH_3CO-LRPGGKKQYKLKHIVGC-NH_2
4	CH_3CO-LKHIVWASRELERFAGC-NH_2
5	CH_3CO-LERFAVNPGLLETSEGC-NH_2
6	CH_3CO-LETSEGSRQILGQLQGC-NH_2
7	CH_3CO-LGQLQPSLQTGSEELGC-NH_2
8	CH_3CO-GSEELRSLYNTIAVLGC-NH_2
9	CH_3CO-TIAVLYSVHQRIDVKGC-NH_2
10	CH_3CO-RIDVKDTKEALDKIEGC-NH_2
11	CH_3CO-LDKIEEEQNKSKKKAGC-NH_2
12	CH_3CO-SKKKAQQAAADTGNNGC-NH_2
13	CH_3CO-DTGNNSQVSQNYGC-NH_2

Figure 1. The construction of MA-based overlapping peptide library.

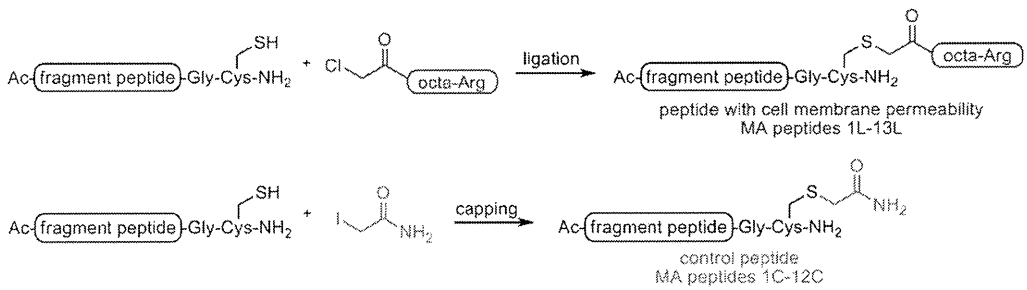

Figure 2. The design of MA peptides with cell membrane permeability (upper) and their control peptides (lower).

residues to preserve secondary structures (Fig. 1). Cys residues of the original MA sequence were changed into Ser residues because of the facility of peptide synthesis. Thirteen MA fragment peptides (1–13) were designed with the addition of Gly as a spacer and Cys as a conjugation site at the C-terminus. To impart cell membrane permeability to these peptides, the N-terminal chloroacetyl group of an octa-arginyl (R_8) peptide[19] was conjugated to the side-chain thiol group of the Cys residue of the above peptides. This resulted in the MA peptides 1L–13L (Fig. 2). R_8 is a cell membrane permeable motif and its fusion with parent peptides is known to produce bioactive peptides with no significant adverse properties.[12,13,20–24] In addition, the R_8-fusion can increase the solubility of MA

Table 1
Anti-HIV activity and cytotoxicity of control MA peptides

MA peptide	MT-4 cell	PM1/CCR5 cell		MT-4 cell
	NL4-3 (MTT assay) EC_{50}[a] (μM)	NL(AD8) (MTT assay) EC_{50}[a] (μM)	JR-CSF (p24 ELISA) EC_{50}[a] (μM)	(MTT assay) CC_{50}[b] (μM)
1C	>50	ND	ND	>50
2C	17 ± 1.4	1.0	ND	>50
3C	>50	ND	ND	>50
4C	No inhibition at 12.5 μM	ND	ND	14
5C	>50	ND	ND	>50
6C	37 ± 12	24% inhibition at 6.25 μM	25% inhibition at 50 μM	>50
7C	>50	ND	ND	>50
8C	>50	ND	ND	>50
9C	29 ± 1.4	13	8.1	>50
10C	No inhibition at 12.5 μM	ND	ND	17
11C	>50	ND	ND	>50
12C	>50	ND	ND	>50
14C	>50	ND	ND	>50
AZT	0.020	0.459	0.17	>100
SCH-D	ND	0.026	0.0014	ND

X4-HIV-1 (NL4-3 strain)-induced cytopathogenicity in MT-4 cells and R5-HIV-1 (NL(AD8) strain)-induced cytopathogenicity in PM1/CCR5 cells evaluated by the MTT assay, and inhibitory activity against R5-HIV-1 (JR-CSF strain)-induced cytopathogenicity in PM1/CCR5 cells evaluated by the p24 ELISA assay.

[a] EC_{50} values are the concentrations for 50% protection from HIV-1-induced cytopathogenicity in MT-4 cells.

[b] CC_{50} values are the concentrations for 50% reduction of the viability of MT-4 cells. All data are the mean values from at least three independent experiments. ND: not determined.

Table 2
Anti-HIV activity and cytotoxicity of MA peptides with cell membrane permeability

MA peptide	MT-4 cell	PM1/CCR5 cell		MT-4 cell
	NL4-3(MTT assay) EC_{50} (μM)	NL(AD8)(MTT assay) EC_{50} (μM)	JR-CSF(p24 ELISA) EC_{50} (μM)	(MTT assay) CC_{50} (μM)
1L	30	30	40	>50
2L	21 ± 4.2	>31	ND	32 ± 4.2
3L	no inhibition at 25 μM	ND	ND	36
4L	no inhibition at 3.13 μM	ND	ND	3.7
5L	40	42% inhibition at 50 μM	42	>50
6L	40 ± 8.9	49% inhibition at 50 μM	31	>50
7L	35 ± 1.5	37% inhibition at 50 μM	35% inhibition at 50 μM	>50
8L	2.3 ± 0.3	5.8	7.8	9.0 ± 2.4
9L	2.1 ± 0.5	0.43	0.58	5.7 ± 2.1
10L	43 ± 8.5	42% inhibitionat 50 μM	27	>50
11L	18 ± 3.0	17% inhibition at 25 μM	23	>50
12L	41 ± 5.5	30% inhibition at 25 μM	27	>50
13L	20 ± 2.1	0.43	11	>50
14L	no inhibition at 25 μM	ND	ND	36
AZT	0.020	0.459	0.17	>100
SCH-D	ND	0.026	0.0014	ND

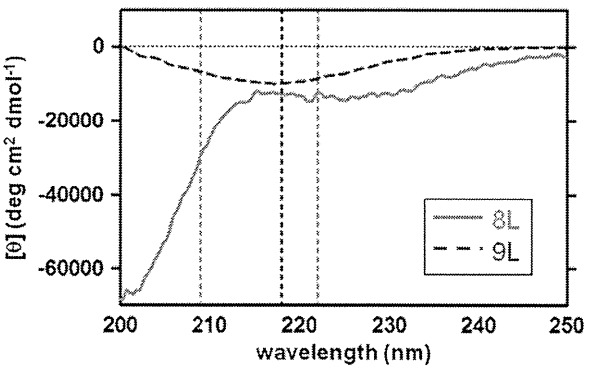

Figure 3. CD spectra of MA peptides 8L (28 μM) and 9L (65 μM) in PBS buffer, pH 7.4 at 25 °C.

peptides whose hydrophobicity is relatively limited. On the other hand, to develop control peptides lacking cell membrane permeability, iodoacetamide was conjugated to the thiol group of the Cys residue to prepare MA peptides 1C–12C (Fig. 2). MA peptide 13C was not synthesized because MA fragment 13 is insoluble in PBS buffer.

The anti-HIV activity of MA peptides 1L–13L and MA peptides 1C–12C, was evaluated. Inhibitory activity against T-cell line-tropic (X4-) HIV-1 (NL4-3 strain)-induced cytopathogenicity in MT-4 cells and against macrophage-tropic (R5-) HIV-1 (NL(AD8) strain)-induced cytopathogenicity in PM1/CCR5 cells was assessed by the 3-[4,5-dimethylthiazol-2-yl]-2,5-diphenyltetrazolium bromide (MTT) assay, and inhibitory activity against R5-HIV-1 (JR-CSF strain) replication in PM1/CCR5 cells was determined by the p24 ELISA assay. The results are shown in Tables 1 and 2. The control MA peptides 6C and 9C showed slight anti-HIV activity against NL4-3, NL(AD8) and JR-CSF strains, and 2C showed high anti-HIV activity against NL4-3 and NL(AD8) strains, but the other control MA peptides showed no significant anti-HIV activity. 2C showed significant anti-HIV activity against both X4-HIV-1 and R5-HIV-1 strains, suggesting that this region of the MA domain is relevant with Gag localization to the plasma membrane (PM)[25] and that 2C might inhibit competitively the interaction between MA and PM. On the other hand, the MA peptides with the exception of 3L and 4L, showed moderate to potent anti-HIV activity against all three strains. These peptides expressed almost the same level of anti-HIV activity against both X4-HIV-1 and R5-HIV-1 strains. The MA peptides 8L and 9L in particular, showed significant anti-HIV activity. These results suggest that MA peptides achieve entry into target cells as a result of the addition of R_8, and inhibit viral replication within the cells. The adjacent peptides 8L and 9L possess an overlapping sequence TIAVL. Such peptides exhibited relatively high cytotoxicity and the MA peptide 4L showed the highest cytotoxicity although it did not show any significant anti-HIV activity. The control MA peptides 1C–12C were relatively weakly cytotoxic. The MA peptides 8C and 9C exhibited no significant cytotoxicity, although the addition of R_8, giving 8L and 9L, caused a remarkable increase in cytotoxicity. This suggests that the octa-arginyl (R_8) sequence is correlated with the

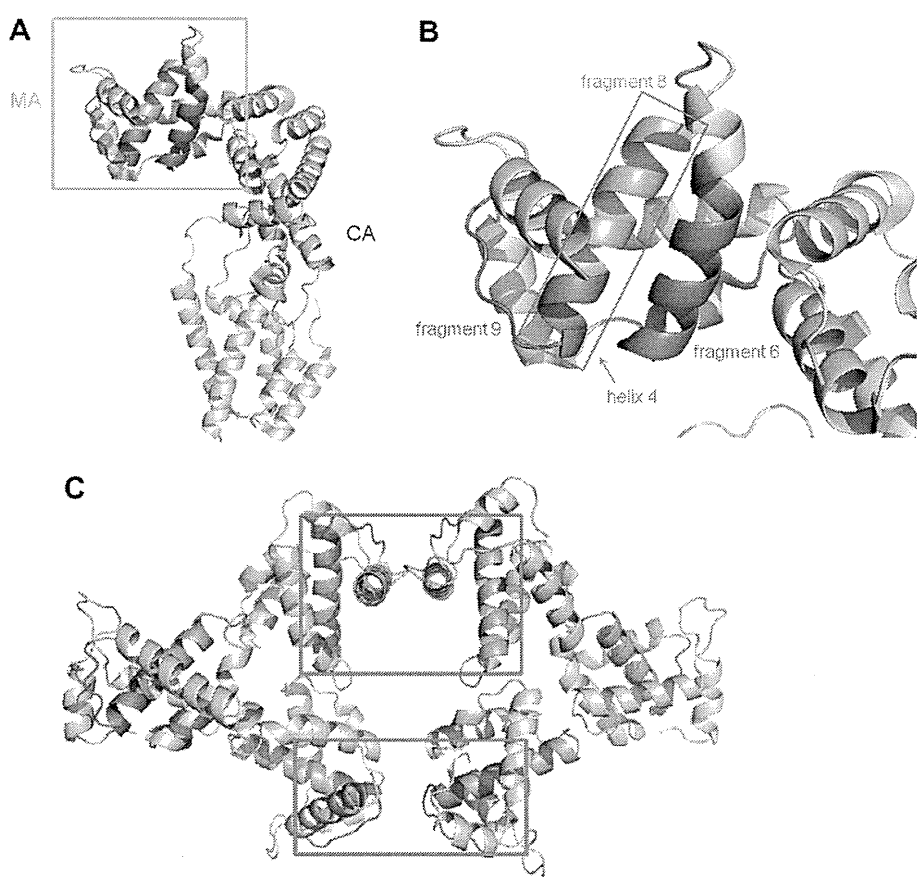

Figure 4. (A) The complete structure of MA and CA proteins (PDB ID: 2gol). (B) The enlarged structure of the highlighted region of (A). (C) The structure of an MA hexamer. Red-colored squares show interfaces between two MA trimers (PDB ID: 1hiw). Orange- and pink-colored helical ribbons represent fragments 8 and 9, respectively.

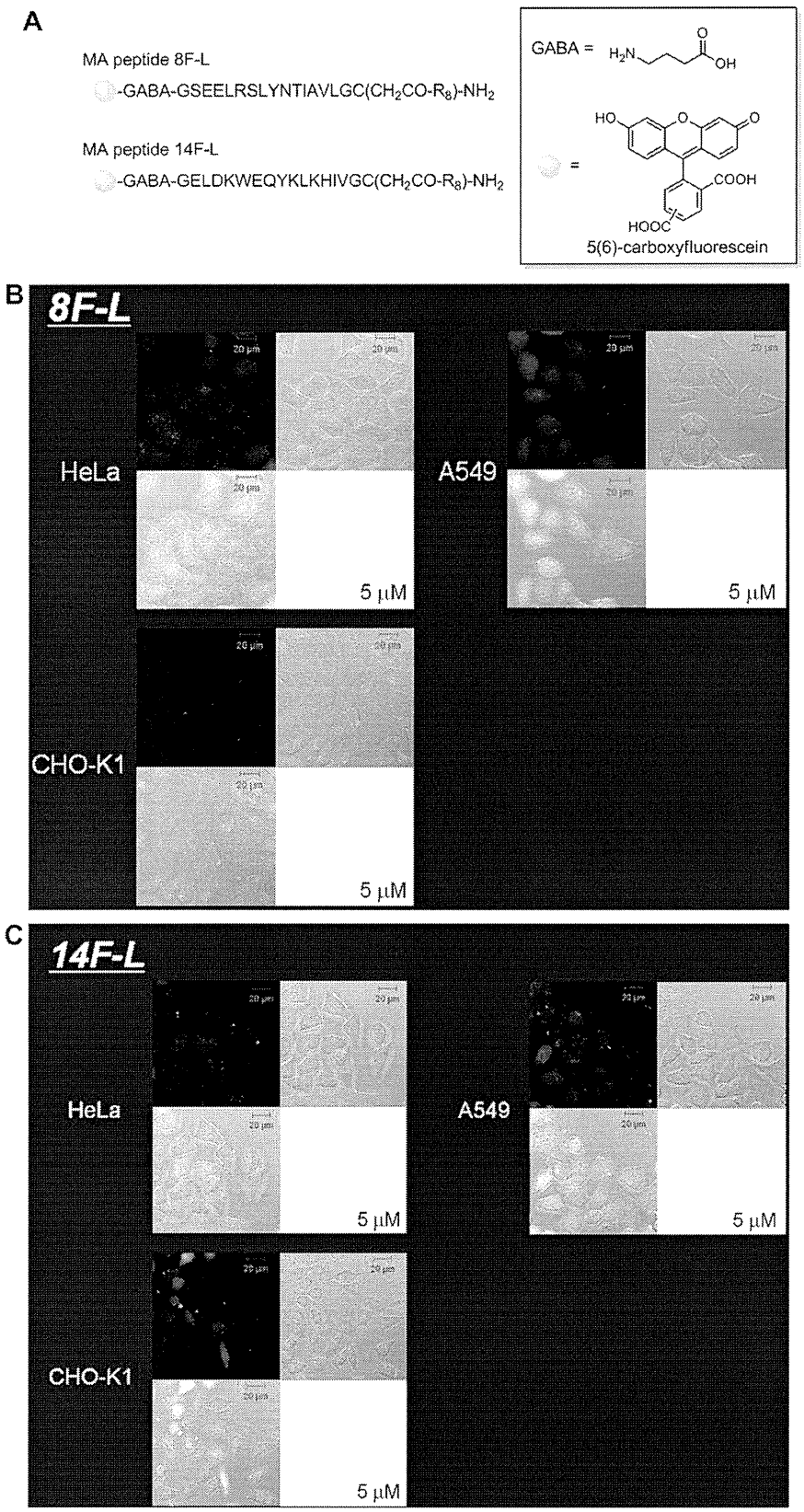

Figure 5. (A) The structures of fluorophore-labeled MA peptides 8F–L and 14F–L. (B) The fluorescent imaging of live cells HeLa, A549 and CHO-K1 by 8F–L. (C) The fluorescent imaging of live cells HeLa, A549 and CHO-K1 by 14F–L.

expression of cytotoxicity and in future, a different effective strategy for cell penetration may be advisable.

In the present assay, the control MA peptides 6C and 9C, which cover MA(51–65) and MA(81–95), respectively, showed significant anti-HIV activity. This is consistent with the previous studies, in which MA(41–55), MA(47–59) and MA(71–85) showed anti-HIV or dimerization inhibitory activity as discussed above.[16–18] These peptides have no R_8 sequence and thus cannot penetrate cell membranes. They exhibit inhibitory activity on the surface of cells, not intracellularly.

The structures of MA peptides 8L and 9L, dissolved in PBS buffer (2.7 mM KCl, 137 mM NaCl, 1.47 mM KH_2PO_4, 9.59 mM Na_2HPO_4) at pH 7.4, were determined by CD spectroscopy (Fig. 3). When peptides form α-helical structures, minima can be observed at approximately 207 and 222 nm in their CD spectra. The amino acid residues covering fragments 8 and 9 corresponding to 8L and 9L are located in an α-helical region (helix 4) of the parent MA protein (Fig. 4), and peptides 8L and 9L were presumed to have an α-helical conformation.[26–28] However, the CD spectra shown in Figure 3, suggest that these peptides lack any characteristic secondary structure. This is because the 15-mer peptide derived from MA is not sufficiently long to form a secondary structure even though Gly, Cys and octa-Arg are attached to their C-terminus. Analysis of the CD spectra suggests MA fragment peptides need a longer sequence in order to form a secondary structure. The CD spectra of the control MA peptides 8C and 9C were not determined because the aqueous solubility of these peptides is inadequate.

Fluorescent imaging of live cells was used to evaluate the cell membrane permeability of the MA peptides 8L and 14L, which showed high and zero significant anti-HIV activity, respectively. The MA fragment 14 is a hybrid of the fragments 2 and 3, and the MA peptides 14L and 14C, which are based on the conjugation of the N-terminal chloroacetyl group of an R_8 peptide and iodoacetamide to the thiol group of the Cys residue, respectively (Supplementary data), are control peptides lacking significant anti-HIV activity (Tables 1 and 2). These peptides were labeled with 5(6)-carboxyfluorescein via a GABA linker at the N-terminus to produce 8F–L and 14F–L (Fig. 5A). The fluorophore-labeled peptides 8F–L and 14F–L were incubated with live cells of HeLa, A549 and CHO-K1, and the imaging was analyzed by a fluorescence microscope (Fig. 5B and C). A549 cells are human lung adenocarcinomic human alveolar basal epithelial cells.[29] Similar penetration of both peptides 8F–L and 14F–L into these cells was observed. Even peptides without significant anti-HIV activity can penetrate cell membranes. The penetration efficiency of both peptides into A549 was relatively high and into HeLa was low. In CHO-K1 the penetration efficiency of 8F–L is relatively low, but that of 14F–L is high. These imaging data confirm that the MA peptides with the R_8 sequence can penetrate cell membranes and suggest that MA peptides such as 8L and 9L should be able to inhibit HIV replication inside cells.

4. Conclusions

Several HIV-1 inhibitory fragment peptides were identified through the screening of an overlapping peptide library derived from the MA protein. Judging by the imaging experiments, peptides possessing the R_8 group can penetrate cell membranes and might exhibit their function intracellularly thus inhibiting HIV replication.

Two possible explanations for the inhibitory activity of these MA fragment peptides can be envisaged: (1) The fragment peptides might attack an MA protein and inhibit the assembly of MA proteins. (2) These peptides might attack a cellular protein and inhibit its interaction with MA. Further studies to elucidate detailed action mechanisms and identify the targets of these peptides will be performed in future. The technique of addition of the R_8 group to peptides enabled us to screen library peptides that function within cells. Thus, the design of an overlapping peptide library of fragment peptides derived from a parent protein with a cell membrane permeable signal is a useful and efficient strategy for finding potent cell-penetrating lead compounds.

In the present study, the MA peptides 8L and 9L were shown to inhibit HIV-1 replication with submicromolar to micromolar EC_{50} values in cells using the MT-4 assay (NL4-3 and NL(AD8) strains) and the p24 ELISA assay (JR-CSF strain). Our findings suggest that these peptides could serve as lead compounds for the discovery of novel anti-HIV agents. Amino acid residues covering fragments 8 and 9 corresponding to 8L and 9L are located in the exterior surface of MA, and in particular in the interface between two MA trimers (Fig. 4C).[26–28] The interaction of two MA trimers leads to the formation of an MA hexamer, which is the MA assembly with physiological significance. Thus, the region covering fragments 8 and 9 is critical to oligomerization of MA proteins. This suggests that MA peptides 8L and 9L might inhibit the MA oligomerization through competitive binding to the parent MA, and that more potent peptides or peptidomimetic HIV inhibitors could result from studies on the mechanism of action of these MA peptides and identification of the interaction sites. Taken together, some seeds for anti-HIV agents are inherent in MA proteins, including inhibitors of the interaction with PM such as the MA peptide 2C.

Acknowledgements

This work was supported in part by Grant-in-Aid for Scientific Research from the Ministry of Education, Culture, Sports, Science, and Technology of Japan, and Health and Labour Sciences Research Grants from Japanese Ministry of Health, Labor, and Welfare. C.H. and T.T. were supported by JSPS Research Fellowships for Young Scientists. The authors thank Ms. M. Kawamata, National Institute of Infectious Diseases, for her assistance in the anti-HIV assay. We also thank Dr. Y. Maeda, Kumamoto University, for providing PM1/CCR5 cells, and Mr. S. Kumakura, Kureha Corporation, for providing SCH-D, respectively.

Supplementary data

Supplementary data associated with this article can be found, in the online version, at doi:10.1016/j.bmc.2011.12.055.

References and notes

1. Ghosh, A. K.; Dawson, Z. L.; Mitsuya, H. *Bioorg. Med. Chem.* **2007**, *15*, 7576.
2. Cahn, P.; Sued, O. *Lancet* **2007**, *369*, 1235.
3. Grinsztejn, B.; Nguyen, B.-Y.; Katlama, C.; Gatell, J. M.; Lazzarin, A.; Vittecoq, D.; Gonzalez, C. J.; Chen, J.; Harvey, C. M.; Isaacs, R. D. *Lancet* **2007**, *369*, 1261.
4. Tamamura, H.; Xu, Y.; Hattori, T.; Zhang, X.; Arakaki, R.; Kanbara, K.; Omagari, A.; Otaka, A.; Ibuka, T.; Yamamoto, N.; Nakashima, H.; Fujii, N. *Biochem. Biophys. Res. Commun.* **1998**, *253*, 877.
5. Fujii, N.; Oishi, S.; Hiramatsu, K.; Araki, T.; Ueda, S.; Tamamura, H.; Otaka, A.; Kusano, S.; Terakubo, S.; Nakashima, H.; Broach, J. A.; Trent, J. O.; Wang, Z.; Peiper, S. C. *Angew. Chem., Int. Ed.* **2003**, *42*, 3251.
6. Tamamura, H.; Hiramatsu, K.; Mizumoto, M.; Ueda, S.; Kusano, S.; Terakubo, S.; Akamatsu, M.; Yamamoto, N.; Trent, J. O.; Wang, Z.; Peiper, S. C.; Nakashima, H.; Otaka, A.; Fujii, N. *Org. Biomol. Chem.* **2003**, *1*, 3663.
7. Tanaka, T.; Nomura, W.; Narumi, T.; Masuda, A.; Tamamura, H. *J. Am. Chem. Soc.* **2010**, *132*, 15899.
8. Yamada, Y.; Ochiai, C.; Yoshimura, K.; Tanaka, T.; Ohashi, N.; Narumi, T.; Nomura, W.; Harada, S.; Matsushita, S.; Tamamura, H. *Bioorg. Med. Chem. Lett.* **2010**, *20*, 354.
9. Narumi, T.; Ochiai, C.; Yoshimura, K.; Harada, S.; Tanaka, T.; Nomura, W.; Arai, H.; Ozaki, T.; Ohashi, N.; Matsushita, S.; Tamamura, H. *Bioorg. Med. Chem. Lett.* **2010**, *20*, 5853.
10. Yoshimura, K.; Harada, S.; Shibata, J.; Hatada, M.; Yamada, Y.; Ochiai, C.; Tamamura, H.; Matsushita, S. *J. Virol.* **2010**, *84*, 7558.

11. Otaka, A.; Nakamura, M.; Nameki, D.; Kodama, E.; Uchiyama, S.; Nakamura, S.; Nakano, H.; Tamamura, H.; Kobayashi, Y.; Matsuoka, M.; Fujii, N. *Angew. Chem., Int. Ed.* **2002**, *41*, 2937.
12. Suzuki, S.; Urano, E.; Hashimoto, C.; Tsutsumi, H.; Nakahara, T.; Tanaka, T.; Nakanishi, Y.; Maddali, K.; Han, Y.; Hamatake, M.; Miyauchi, K.; Pommier, Y.; Beutler, J. A.; Sugiura, W.; Fuji, H.; Hoshino, T.; Itotani, K.; Nomura, W.; Narumi, T.; Yamamoto, N.; Komano, J. A. *J. Med. Chem.* **2010**, *53*, 5356.
13. Suzuki, S.; Maddali, K.; Hashimoto, C.; Urano, E.; Ohashi, N.; Tanaka, T.; Ozaki, T.; Arai, H.; Tsutsumi, H.; Narumi, T.; Nomura, W.; Yamamoto, N.; Pommier, Y.; Komano, J. A.; Tamamura, H. *Bioorg. Med. Chem.* **2010**, *18*, 6771.
14. Freed, E. O. *Virology* **1998**, *251*, 1.
15. Bukrinskaya, A. *Virus Res.* **2007**, *124*, 1.
16. Niedrig, M.; Gelderblom, H. R.; Pauli, G.; März, J.; Bickhard, H.; Wolf, H.; Modrow, S. *J. Gen. Virol.* **1994**, *75*, 1469.
17. Cannon, P. M.; Matthews, S.; Clark, N.; Byles, E. D.; Iourin, O.; Hockley, D. J.; Kingsman, S. M.; Kingsman, A. J. *J. Virol.* **1997**, *71*, 3474.
18. Morikawa, Y.; Kishi, T.; Zhang, W. H.; Nermut, M. V.; Hockley, D. J.; Jones, I. M. *J. Virol.* **1995**, *69*, 4519.
19. Suzuki, T.; Futaki, S.; Niwa, M.; Tanaka, S.; Ueda, K.; Sugiura, Y. *J. Biol. Chem.* **2002**, *277*, 2437.
20. Wender, P. A.; Mitchell, D. J.; Pattabiraman, K.; Pelkey, E. T.; Steinman, L.; Rothbard, J. B. *Proc. Natl. Acad. Sci. U.S.A.* **2000**, *97*, 13003.
21. Matsushita, M.; Tomizawa, K.; Moriwaki, A.; Li, S. T.; Terada, H.; Matsui, H. *J. Neurosci.* **2001**, *21*, 6000.
22. Takenobu, T.; Tomizawa, K.; Matsushita, M.; Li, S. T.; Moriwaki, A.; Lu, Y. F.; Matsui, H. *Mol. Cancer Ther.* **2002**, *1*, 1043.
23. Wu, H. Y.; Tomizawa, K.; Matsushita, M.; Lu, Y. F.; Li, S. T.; Matsui, H. *Neurosci. Res.* **2003**, *47*, 131.
24. Rothbard, J. B.; Garlington, S.; Lin, Q.; Kirschberg, T.; Kreider, E.; McGrane, P. L.; Wender, P. A.; Khavari, P. A. *Nat. Med.* **2000**, *6*, 1253.
25. Ono, A. *J. Virol.* **2004**, *78*, 1552.
26. Rao, Z.; Belyaev, A. S.; Fry, E.; Roy, P.; Jones, I. M.; Stuart, D. I. *Nature* **1995**, *378*, 743.
27. Hill, C. P.; Worthylake, D.; Bancroft, D. P.; Christensen, A. M.; Sundquist, W. I. *Proc. Natl. Acad. Sci. U.S.A.* **1996**, *93*, 3099.
28. Kelly, B. N.; Howard, B. R.; Wang, H.; Robinson, H.; Sundquist, W. I.; Hill, C. P. *Biochemistry* **2006**, *45*, 11257.
29. Murdoch, C.; Monk, P. N.; Finn, A. *Immunology* **1999**, *98*, 36.